Electronic Supporting Information

Controlled Aggregation Properties of Single Amino Acids Modified with Protecting Groups

Bharti Koshti[+a], Vivekshinh Kshtriya[+a], Soumick Naskar[+a], Hanuman Narode[a], Nidhi Gour[a]*

[a] Department of Chemistry, Indrashil University, Kadi, Mehsana, Gujarat, India; E-mail: gournidhi@gmail.com; nidhi.gour@indrashiluniversity.edu.in

[+] Equal Contribution

Materials and Methods:

Co-incubation studies of modified aliphatic and aromatic single amino acids with dyes: Co-incubation study of modified aliphatic and aromatic single amino acids was done by using fluoresceine and rhodamine B dye. For this study, 10 µM dye was co-incubated with various concentration of modified single amino acids at room temperature as well as on heating at 70 ^{0}C. The solution was dispensed on a clean glass slide and dried at room temperature. All the samples were visualized under Leica DM2500 upright fluorescence microscope under bright field, green filter (Ex 480/40; Em 527/30) and red filter (Ex 546/10; Em 585/40).

Co-incubation studies of modified aliphatic and aromatic amino acids with tannic acid (TA) and urea: Co-incubation studies of modified aliphatic and aromatic single amino acids was done by increasing the concentration of tannic acid and urea in different ratios and keeping the concentration of amino acids constant. Hence, we co-incubated all modified single amino acids at 1:1, 1:3 and 1:5 ratio. A 20 µL co-incubated solution was dispensed on a clean glass slide and dried at room temperature. The images were visualized under Leica DM2500 upright fluorescence microscope under bright field at various magnifications.

UV-Visible spectroscopy studies

For UV-Visible study of all the modified single amino acids, a 50 mM stock solution of modified single amino acids was prepared in methanol. Further dilution was carried out at final concentrations 10 μM, 50 μM, 100 μM using milli-Q water. The UV-visible spectra were recorded on Specord@270 plus, analytikjena, Germany.

Fluorescence Spectroscopy

The fluorescence spectra of all modified single amino acids were recorded using JASCO FP-8300 spectrofluorometer by giving excitation bandwidth 1 nm and emission bandwidth 2.5 nm respectively. The emission spectra of all modified single amino acids were recorded by diluting the 50 mM stock solution (in methanol) of modified single amino acids in milli-Q water to 50 μM and 100 μM final concentrations. The emission spectra of all modified single amino acids were recorded by giving an excitation wavelength 290 nm and recording its emission in range of 300 to 600 nm.

Dynamic Light Scattering (DLS)

Dynamic light scattering was performed at 25 ^{0}C on Malvern Zetasizer version 7.3 with 632.8 nm laser at 90u scattering angle. 100 μM solution of all modified single amino acids was prepared in Milli-Q water and passed it through 0.2 mm filter and kept at room temperature for 5 minutes. Subsequently the DLS spectra were recorded.

Turbidity Assay

The turbidity assay were performed at varying concentration of **Fmoc-Lys(Boc)-OH**, **Fmoc-Glu(OtBu)-OH**, **Fmoc-Asp(OtBu)-OH**, and **Fmoc-Tyr(tBu)-OH**, in milli-Q water from 5 to 200 μM. While in case of **Cbz-Phe-OH** and **Cbz-Trp-OH** the turbidity assays were performed at 5 μM to 10 mM concentration due to lesser turbidity of these modified single

amino acids at lower concentration. The all the modified single amino acid shows the no turbidity at lower concentration but as we alter the concentrations turbidity were increases in modified single amino acids. The full UV-visible spectrum was recorded on UV-1900 SHIMADZU spectrophotometer, and plot the graph absorbance versus concentration at 440 nm for each modified single amino acid.

X-Ray Diffraction (XRD)

X-ray diffraction experiments were performed on Bruker AXS D8 Focus P-XRD Bruker and AXS D8 VENTURE SC-XRD. All modified single amino acids were evenly dispersed over the substrate holder and scanned in the range of 2θ 10-80°. The non-assembled samples used were commercially available **Fmoc-Lys(Boc)-OH** and **Cbz-Phe-OH** used as such while the assembled samples for XRD were prepared by lyophilizing these modified single amino acids at 3 mM and 10 mM concentration which was prior incubated for 24h at RT in de-ionized water and thereafter lyophilized in Scale Bench Top Freeze Dryer. The lyophilized powder thus obtained was used further for XRD analysis.

Concentration-dependent ^{1}H-NMR spectroscopy

^{1}H-NMR spectra were recorded on a 400 MHz NMR spectrometer at 25 °C. The concentration-dependent ^{1}H-NMR spectra were recorded at 1, 3, 5, 7 and 9 mg/mL concentrations in DMSO-d6 and subsequently addition of drop of D_2O in **Fmoc-Lys(Boc)-OH** and **Cbz-Phe-OH**. The FID files of ^{1}H NMR processed by using the mestReNova version 6.0.2-5475 software.

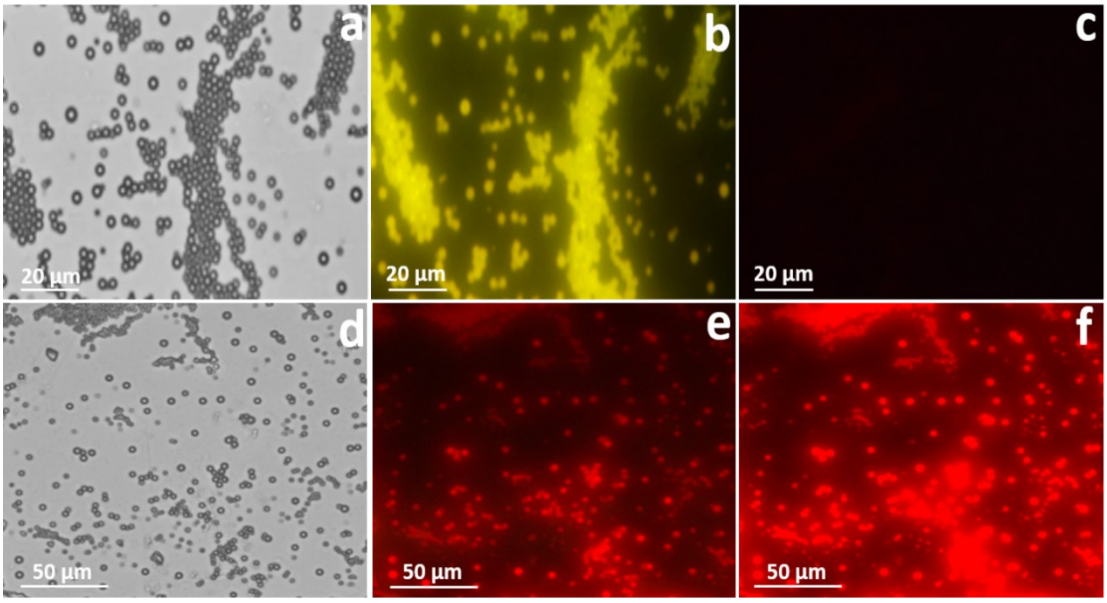

Fig. S1 Microscopy images of **Fmoc-Lys(Boc)-OH** (10 mM) after heating at 70 °C and thereafter co-incubated with 10 µM dye (a) with fluoresceine dye under bright field; (b) with fluoresceine dye under green filter; (c) with fluoresceine dye under red filter; (d) with rhodamine B dye under bright field; (e) with rhodamine B dye under green filter; (f) with rhodamine B dye under red filter.

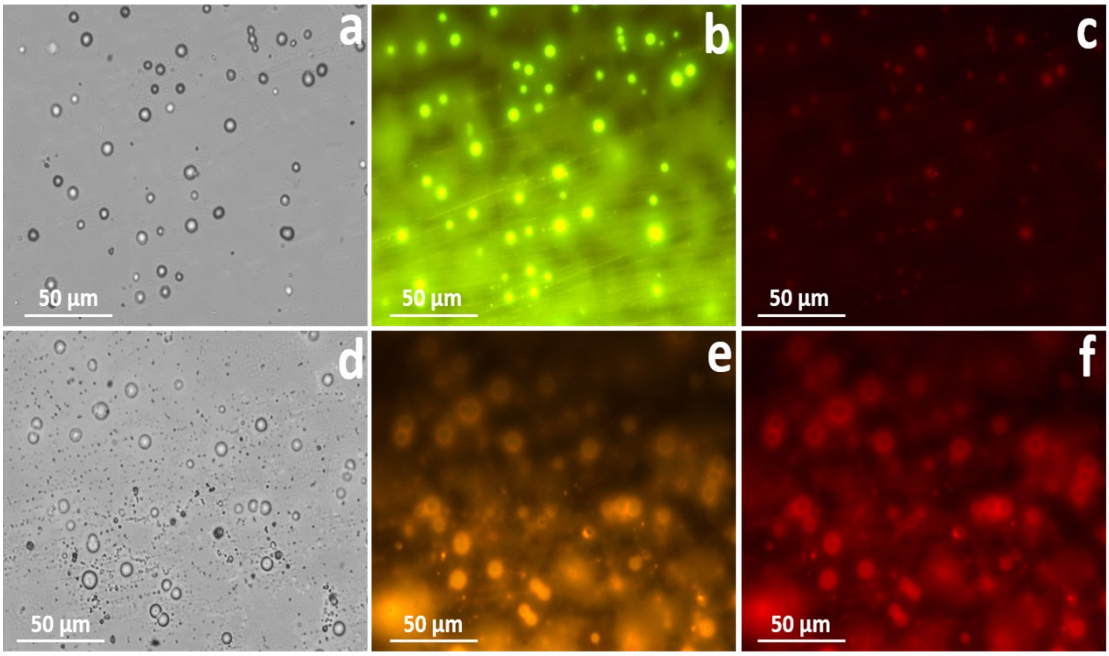

Fig. S2 Microscopy images of **Fmoc-Glu(OtBu)-OH** (3 mM) at room temperature when co-incubated with 10 µM microscopic dye (a) with fluoresceine dye under bright field; (b) with fluoresceine dye under green filter; (c) with fluoresceine dye under red filter; (d) with rhodamine B dye under bright field; (e) with rhodamine B dye under green filter; (f) with rhodamine B dye under red filter.

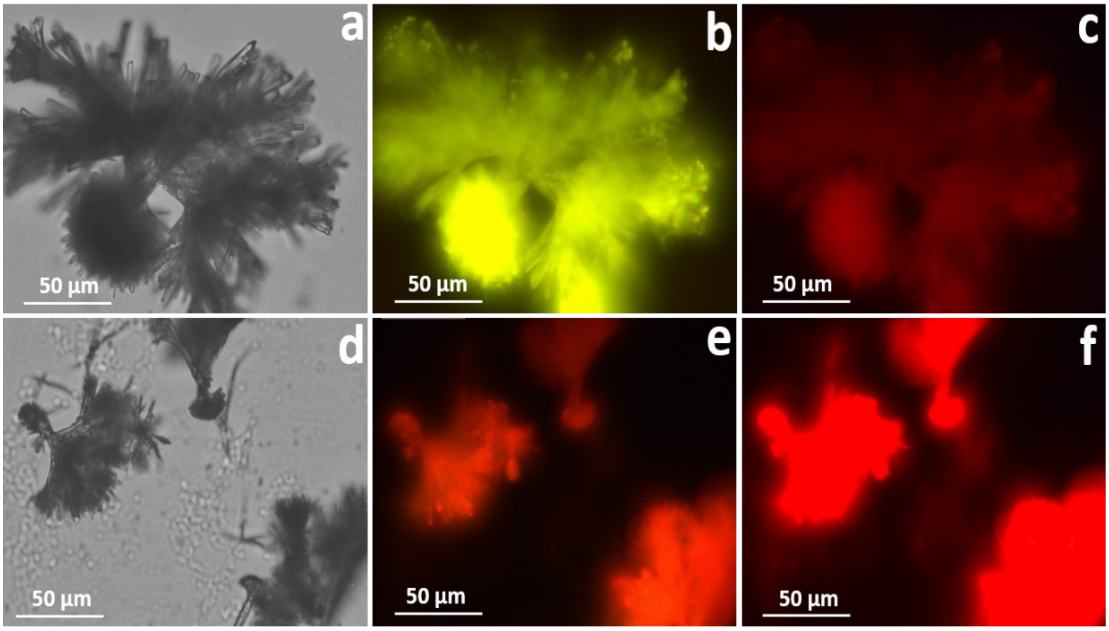

Fig. S3 Microscopy images of **Fmoc-Glu(OtBu)-OH** (10 mM) after heating at 70 °C thereafter co-incubated with 10 µM dye (a) with fluoresceine dye under bright field; (b) with fluoresceine dye under green filter; (c) with fluoresceine dye under red filter; (d) with rhodamine B dye under bright field; (e) with rhodamine B dye under green filter; (f) with rhodamine B dye under red filter.

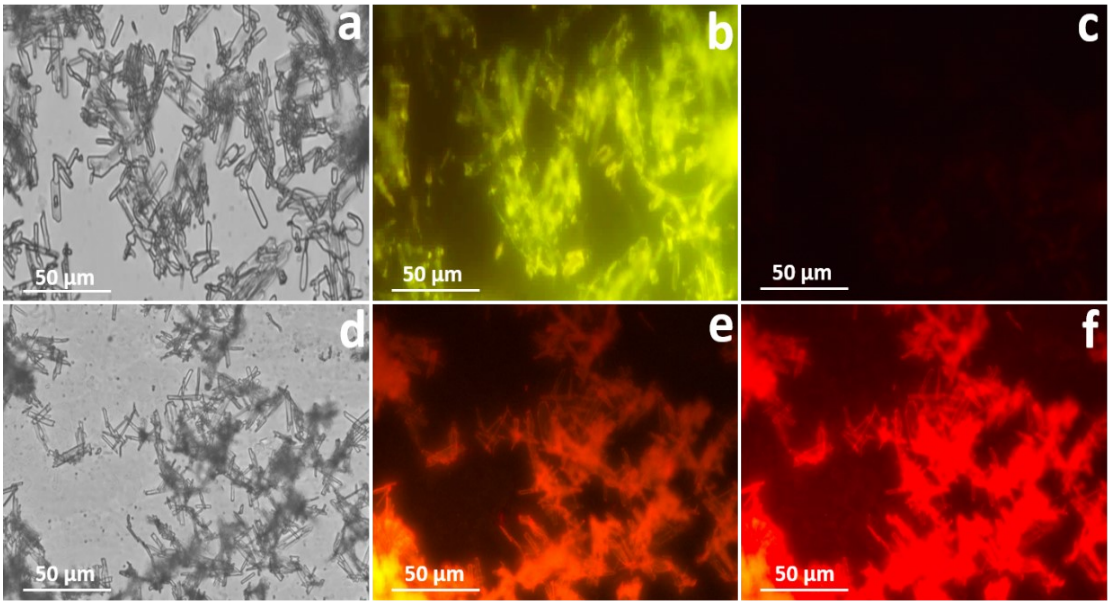

Fig. S4 Microscopy images of **Fmoc-Asp(OtBu)-OH** (3 mM) at room temperature when co-incubated with 10 µM microscopic dye (a) with fluoresceine dye under bright field; (b) with fluoresceine dye under green filter; (c) with fluoresceine dye under red filter; (d) with rhodamine B dye under bright field; (e) with rhodamine B dye under green filter; (f) with rhodamine B dye under red filter.

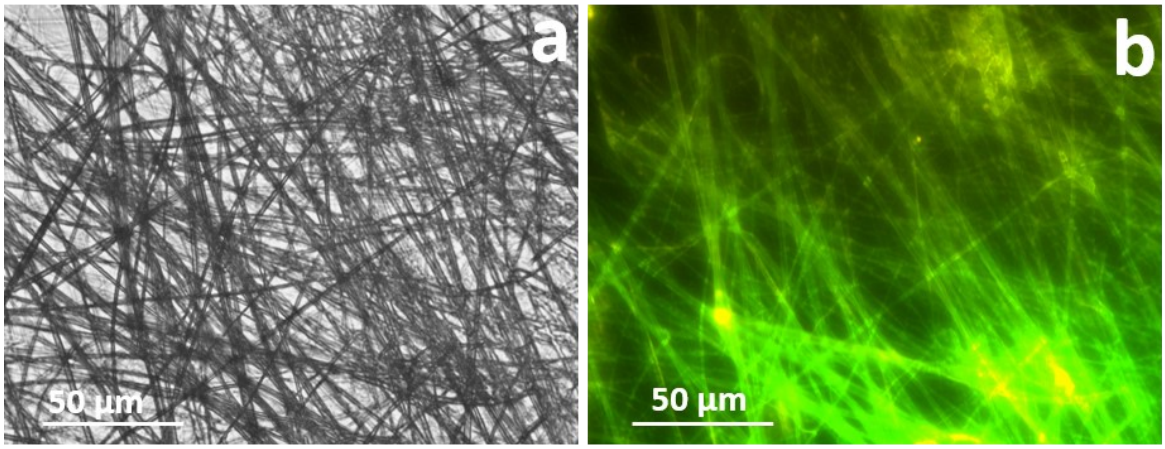

Fig S5 Microscopy images of **Cbz-Phe-OH** (3 mM) on binding with thioflavin T (a) under bright filed; (b) with ThT under green filter.

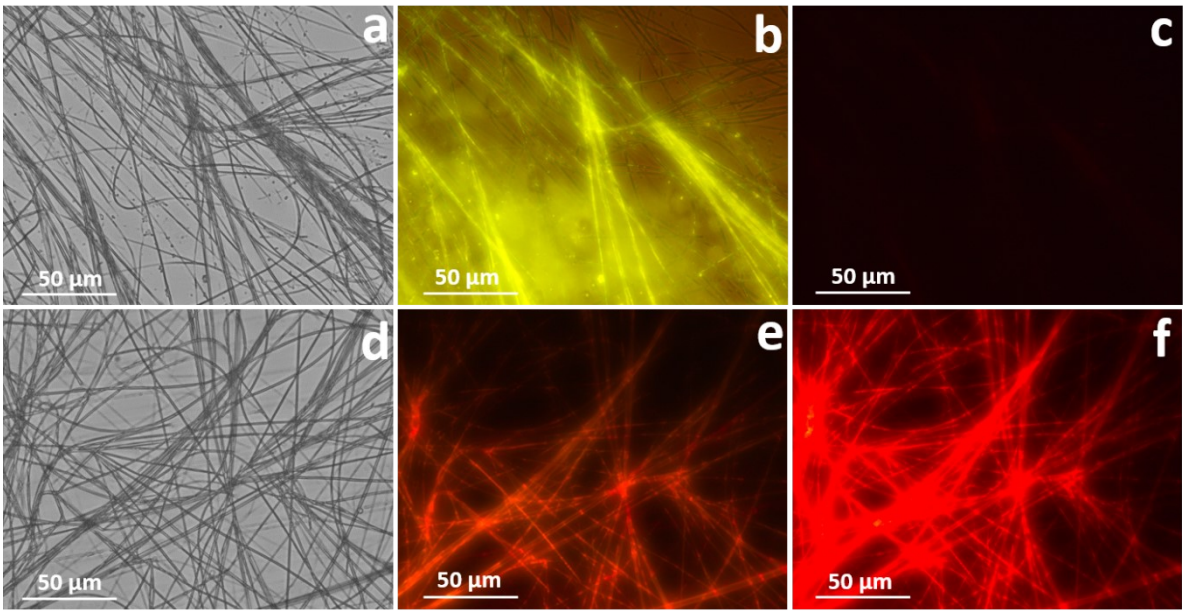

Fig. S6 Microscopy images of **Cbz-Phe-OH** (3 mM) under room temperature condition when co-incubated with 10 µM microscopic dye (a) with fluoresceine dye under bright field; (b) with fluoresceine dye under green filter; (c) with fluoresceine dye under red filter; (d) with rhodamine B dye under bright field; (e) with rhodamine B dye under green filter; (f) with rhodamine B dye under red filter.

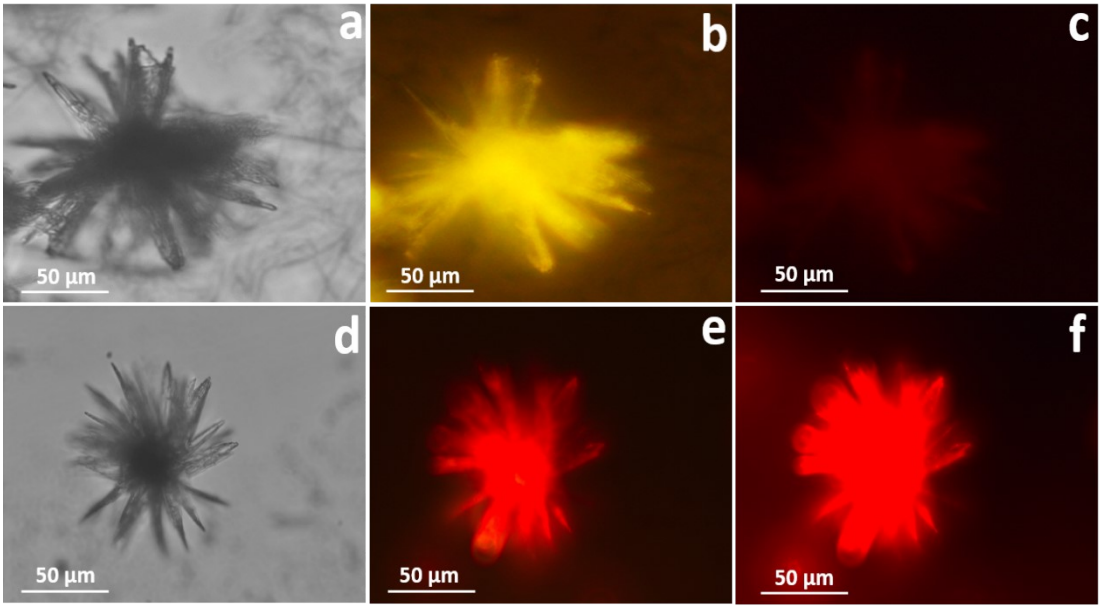

Fig. S7 Microscopy images of **Cbz-Trp-OH** (3 mM) under room temperature condition when co-incubated with 10 µM microscopic dye (a) with fluoresceine dye under bright field; (b) with fluoresceine dye under green filter; (c) with fluoresceine dye under red filter; (d) with rhodamine B dye under bright field; (e) with rhodamine B dye under green filter; (f) with rhodamine B dye under red filter.

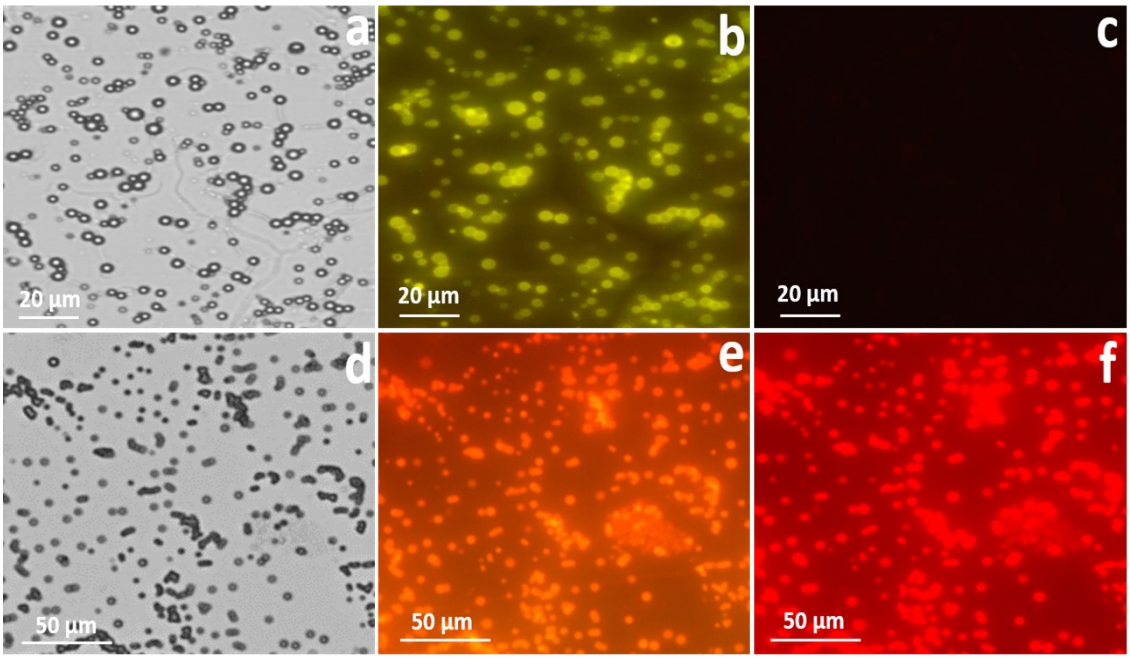

Fig. S8 Microscopy images of **Fmoc-Tyr(tBu)-OH** (3 mM) under room temperature condition when co-incubated with 10 µM microscopic dye (a) with fluoresceine dye under bright field; (b) with fluoresceine dye under green filter; (c) with fluoresceine dye under red filter; (d) with rhodamine B dye under bright field; (e) with rhodamine B dye under green filter; (f) with rhodamine B dye under red filter.

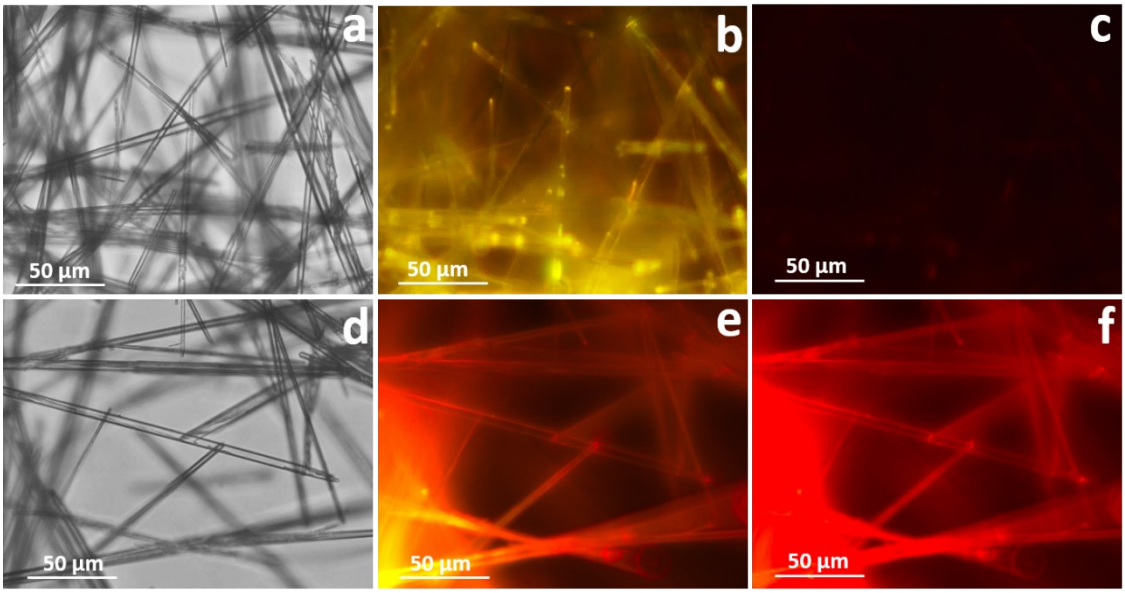

Fig. S9 Microscopy images of **Fmoc-Tyr(tBu)-OH** (3 mM) after heating at 70 °C and thereafter co-incubated with 10 µM microscopic dye (a) with fluoresceine dye under bright field; (b) with fluoresceine dye under green filter; (c) with fluoresceine dye under red filter; (d) with rhodamine B dye under bright field; (e) with rhodamine B dye under green filter; (f) with rhodamine B dye under red filter.

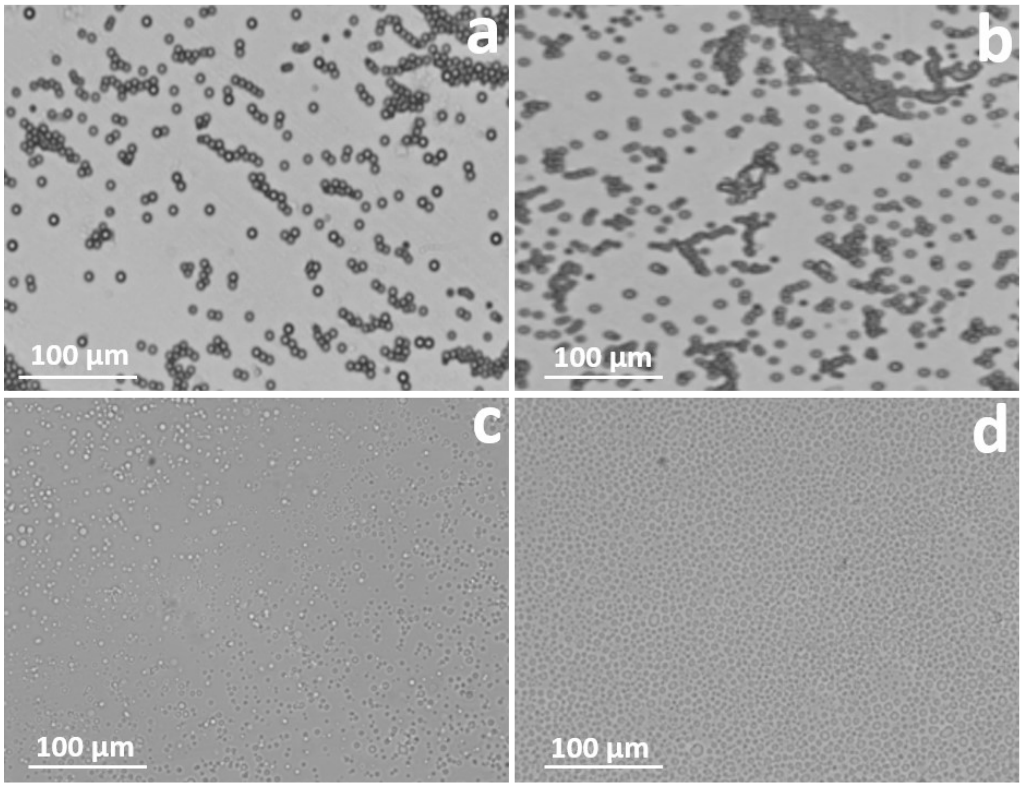

Fig. S10 Optical microscopy images of **Fmoc-Lys(Boc)-OH** (10 mM) after heating at 70 ^{0}C and thereafter co-incubated with tannic acid (a) **Fmoc-Lys(Boc)-OH** under bright field; (b) with tannic acid in 1:1 ratio; (c) with tannic acid in 1:3 ratio; (d) with tannic acid in 1:5 ratio.

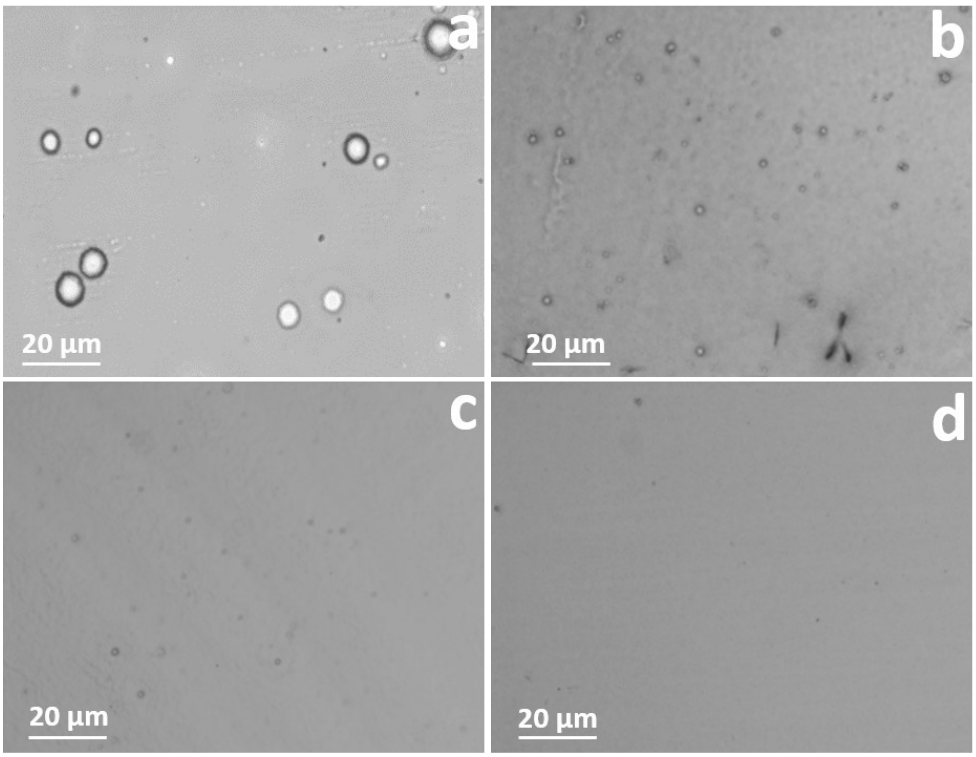

Fig. S11 Optical microscopy images of **Fmoc-Glu(OtBu)-OH** (3 mM) at RT when co-incubated with tannic acid (a) **Fmoc-Glu(OtBu)-OH** under bright field; (b) with tannic acid in 1:1 ratio; (c) with tannic acid in 1:3 ratio; (d) with tannic acid in 1:5 ratio.

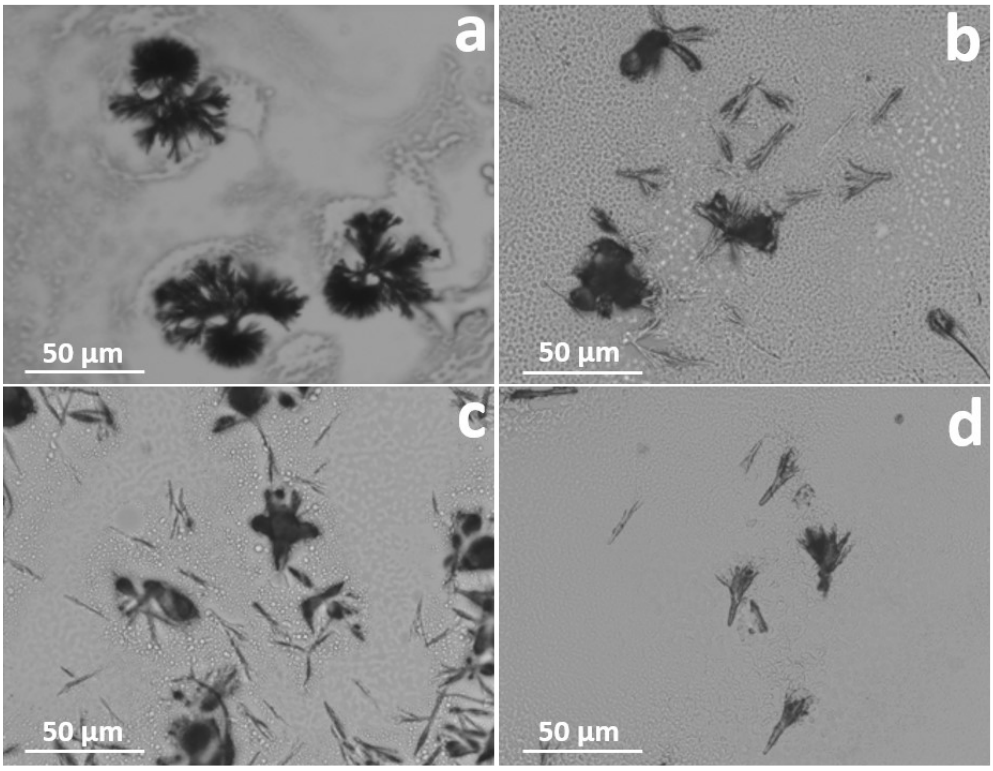

Fig. S12 Optical microscopy images of **Fmoc-Glu(OtBu)-OH** (10 mM) after heating at 70 °C and thereafter co-incubated with tannic acid (a) **Fmoc-Glu(OtBu)-OH** under bright field; (b) with tannic acid in 1:1 ratio; (c) with tannic acid in 1:3 ratio; (d) with tannic acid in 1:5 ratio.

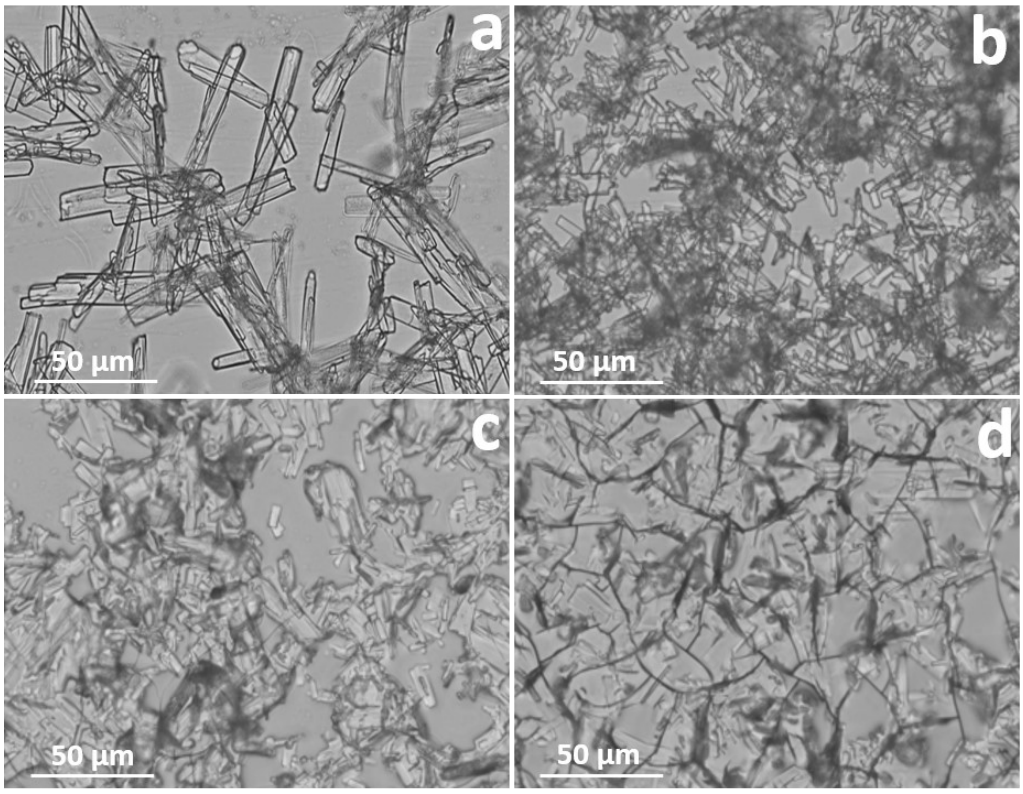

Fig. S13 Optical microscopy images of **Fmoc-Asp(OtBu)-OH** (3 mM) at RT when co-incubated with tannic acid (a) **Fmoc-Asp(OtBu)-OH** under bright field; (b) with tannic acid in 1:1 ratio; (c) with tannic acid in 1:3 ratio; (d) with tannic acid in 1:5 ratio.

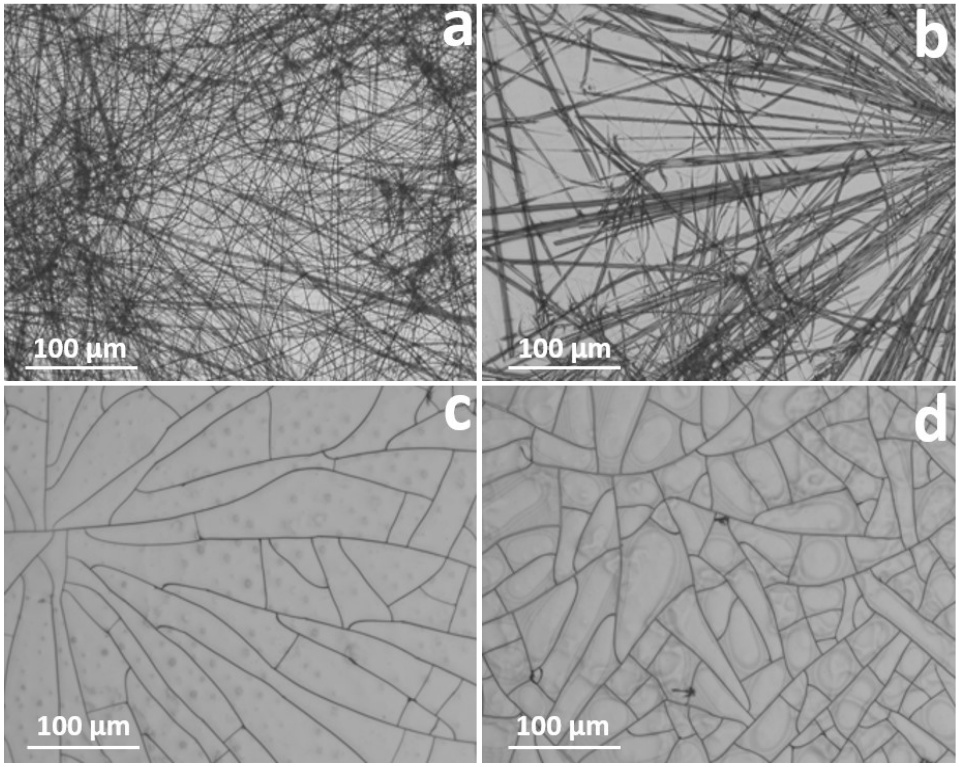

Fig. S14 Optical microscopy images of **Cbz-Phe-OH** (3 mM) at RT when co-incubated with tannic acid (a) **Cbz-Phe-OH** under bright field; (b) with tannic acid in 1:1 ratio; (c) with tannic acid in 1:3 ratio; (d) with tannic acid in 1:5 ratio.

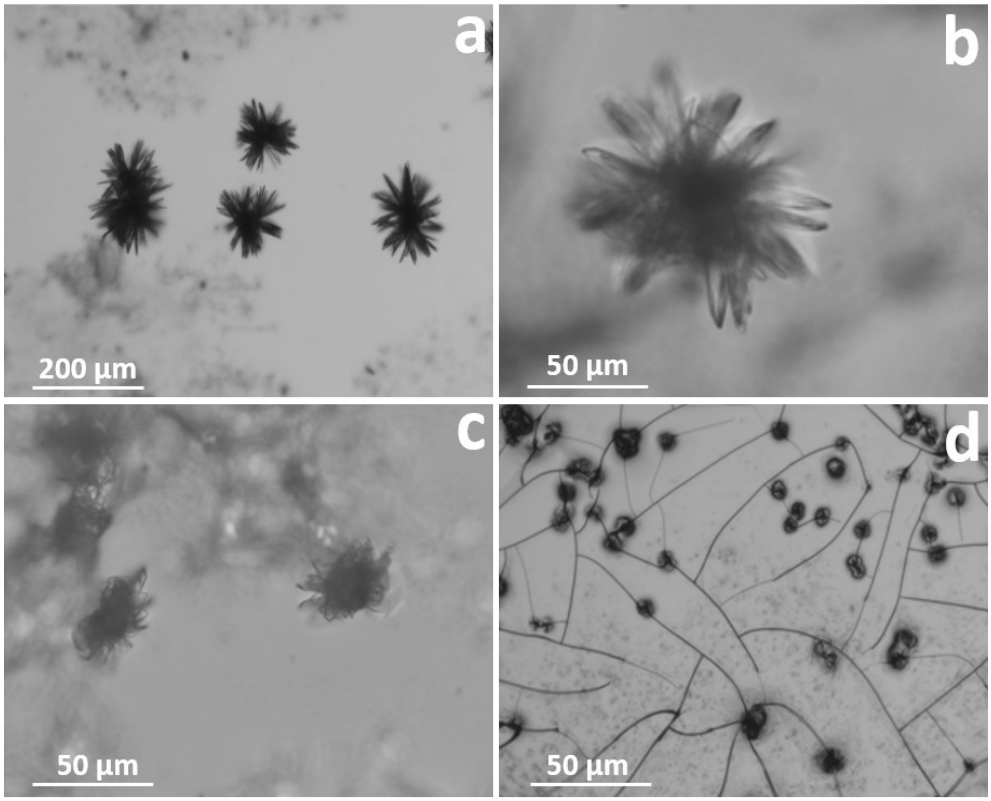

Fig. S15 Optical microscopy images of **Cbz-Trp-OH** (3 mM) at RT when co-incubated with tannic acid (a) **Cbz-Trp-OH** under bright field; (b) with tannic acid in 1:1 ratio; (c) with tannic acid in 1:3 ratio; (d) with tannic acid in 1:5 ratio.

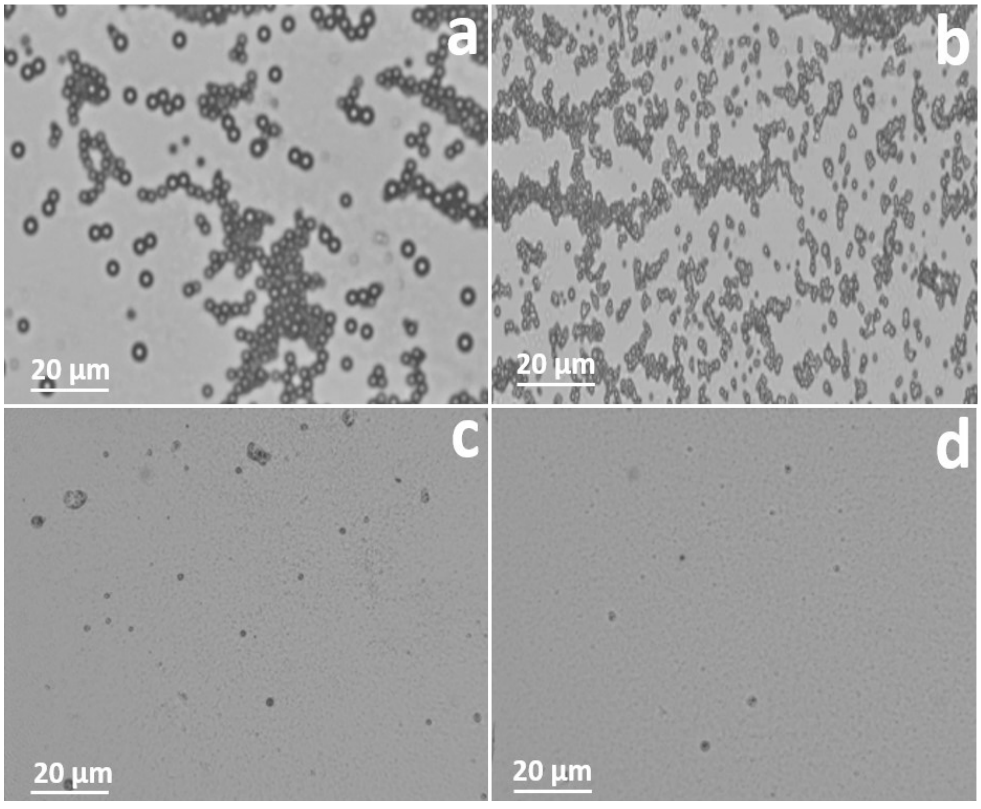

Fig. S16 Optical microscopy images of **Fmoc-Tyr(tBu)-OH** (3 mM) at RT when co-incubated with tannic acid (a) **Fmoc-Tyr(tBu)-OH** under bright field; (b) with tannic acid in 1:1 ratio; (c) with tannic acid in 1:3 ratio; (d) with tannic acid in 1:5 ratio.

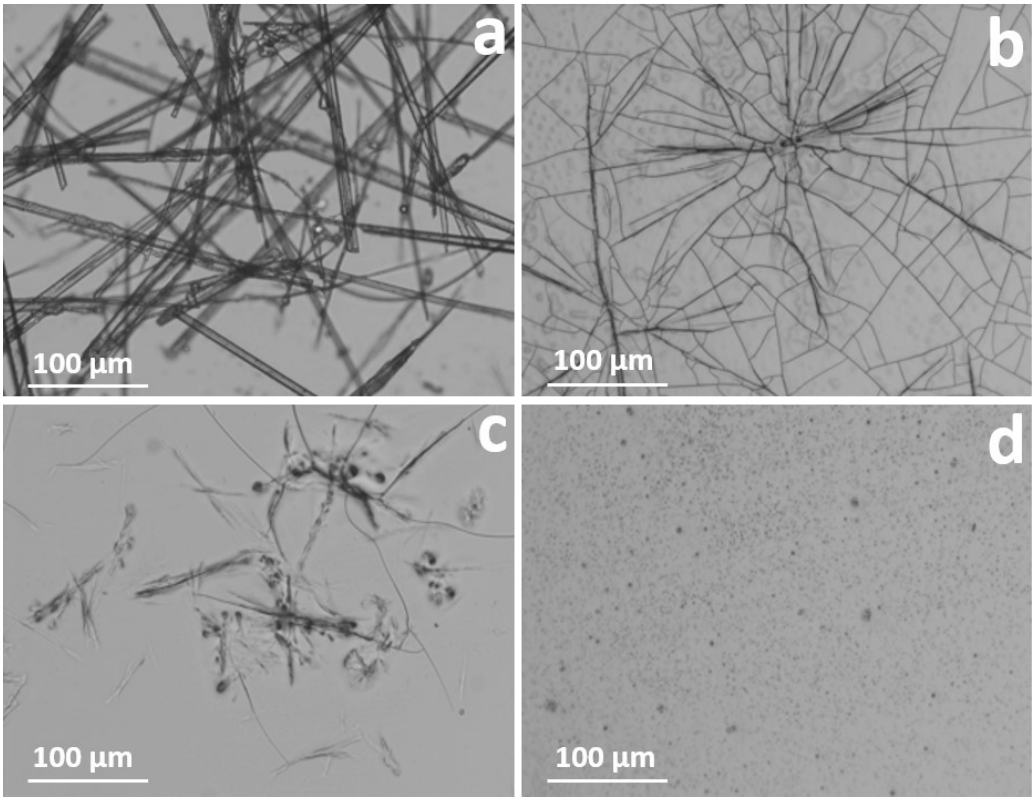

Fig. S17 Optical microscopy images of **Fmoc-Tyr(tBu)-OH** (3 mM) after heating at 70 °C and thereafter co-incubated with tannic acid (a) **Fmoc-Tyr(tBu)-OH** under bright field; (b) with tannic acid in 1:1 ratio; (c) with tannic acid in 1:3 ratio; (d) with tannic acid in 1:5 ratio.

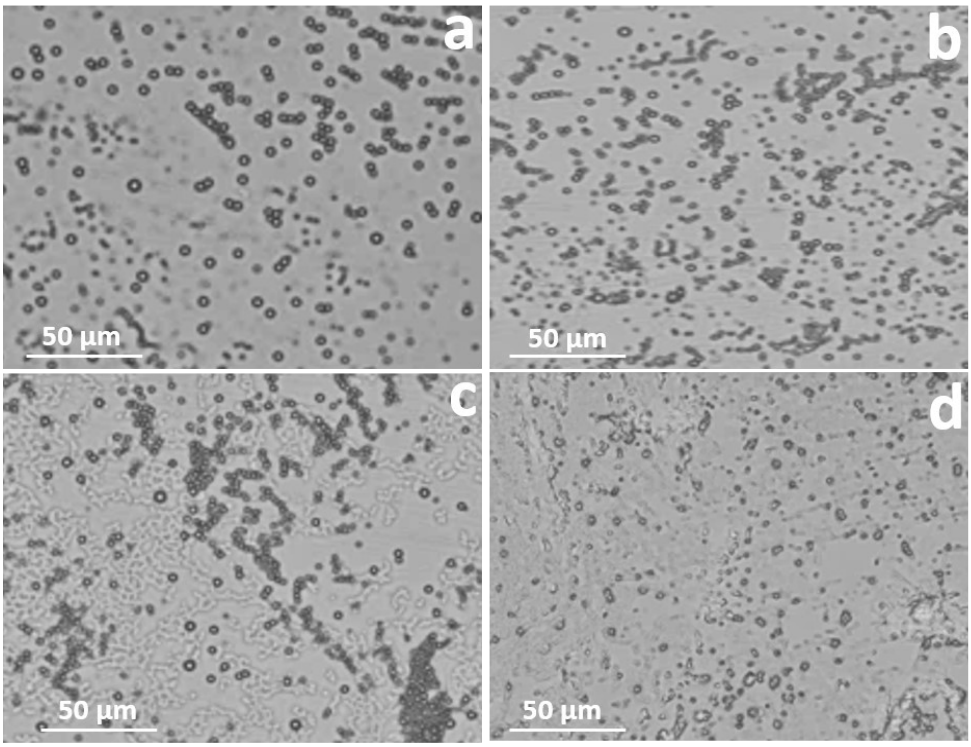

Fig. S18 Optical microscopy images of **Fmoc-Lys(Boc)-OH** (10 mM) on heating at 70 °C when co-incubated with urea (a) **Fmoc-Lys(Boc)-OH** under bright field; (b) with urea in 1:1 ratio; (c) with urea in 1:3 ratio; (d) with urea in 1:5 ratio.

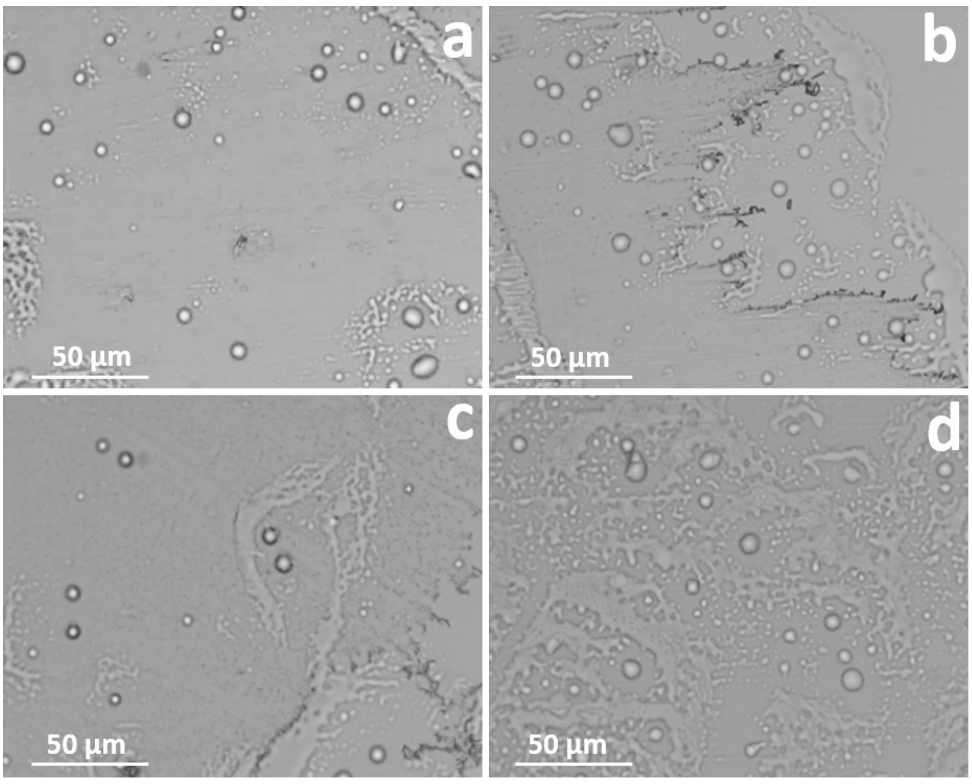

Fig. S19 Optical microscopy images of **Fmoc-Glu(OtBu)-OH** (3 mM) at RT when co-incubated with urea (a) **Fmoc-Glu(OtBu)-OH** under bright field; (b) with urea in 1:1 ratio; (c) with urea in 1:3 ratio; (d) with urea in 1:5 ratio.

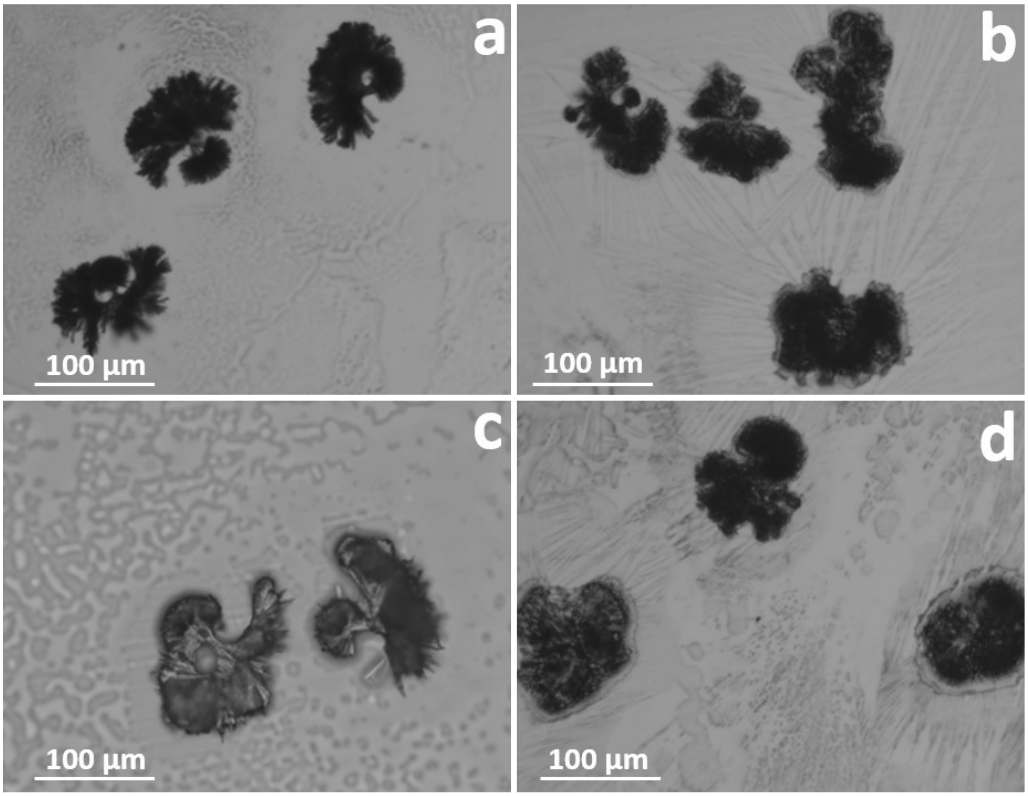

Fig. S20 Optical microscopy images of **Fmoc-Glu(OtBu)-OH** (10 mM) on heating at 70 ^{o}C when co-incubated with urea (a) **Fmoc-Glu(OtBu)-OH** under bright field; (b) with urea in 1:1 ratio; (c) with urea in 1:3 ratio; (d) with urea in 1:5 ratio.

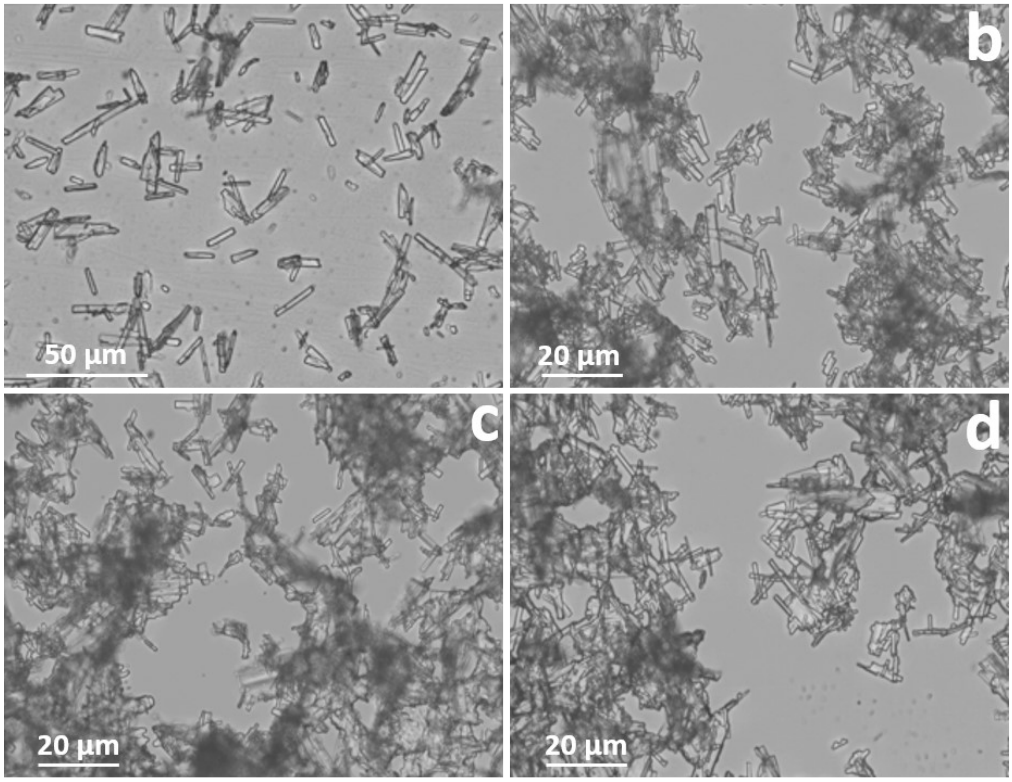

Fig. S21 Optical microscopy images of **Fmoc-Asp(OtBu)-OH** (3 mM) at RT when co-incubated with urea (a) **Fmoc-Asp(OtBu)-OH** under bright field; (b) with urea in 1:1 ratio; (c) with urea in 1:3 ratio; (d) with urea 1:5 ratio.

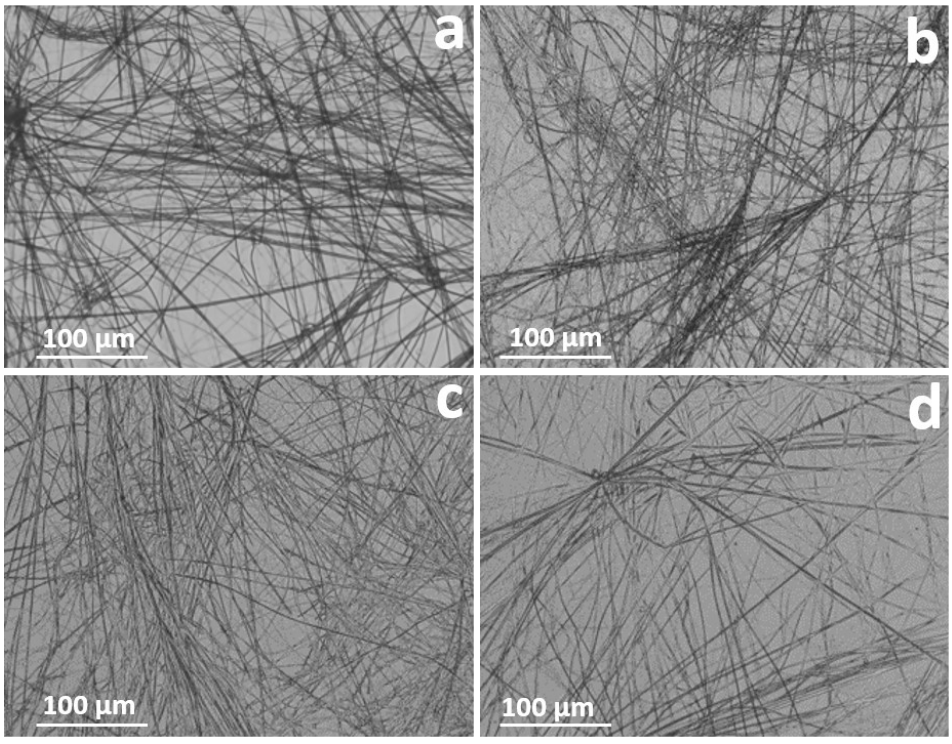

Fig. S22 Optical microscopy images of **Cbz-Phe-OH** (3 mM) at RT when co-incubated with urea (a) **Cbz-Phe-OH** under bright field; (b) with urea in 1:1 ratio; (c) with urea in 1:3 ratio; (d) with urea 1:5 ratio.

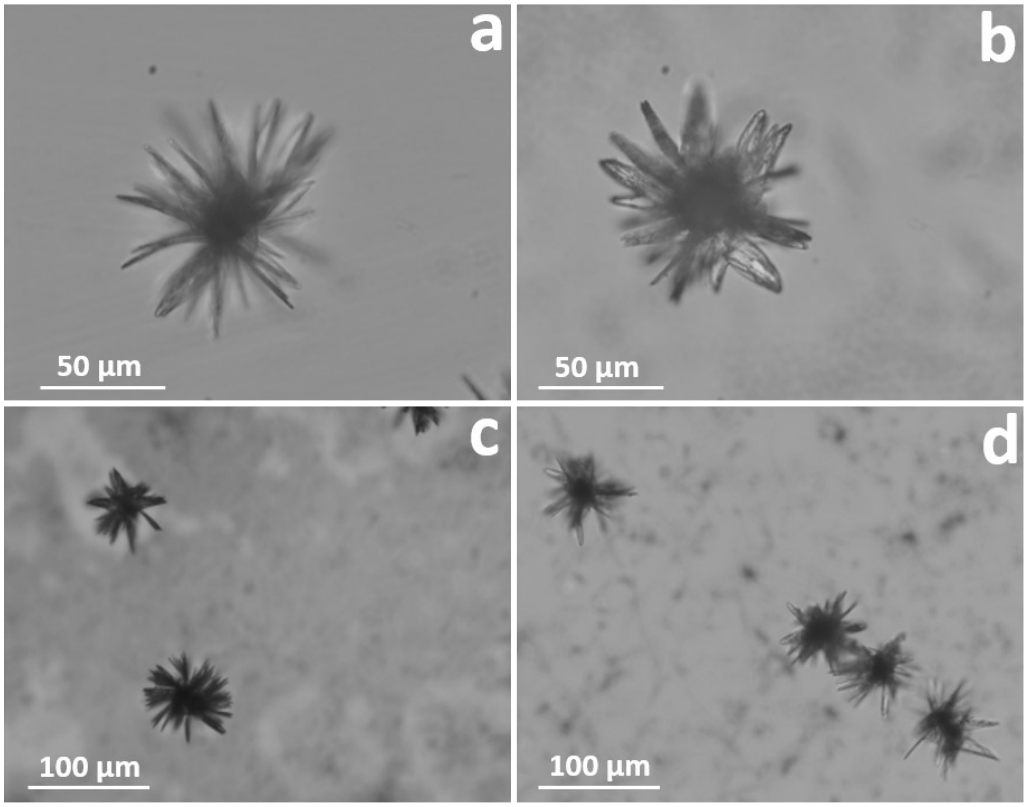

Fig. S23 Optical microscopy images of **Cbz-Trp-OH** (3 mM) at RT when co-incubated with urea (a) **Cbz-Trp-OH** under bright field; (b) with urea in 1:1 ratio; (c) with urea in 1:3 ratio; (d) with urea 1:5 ratio.

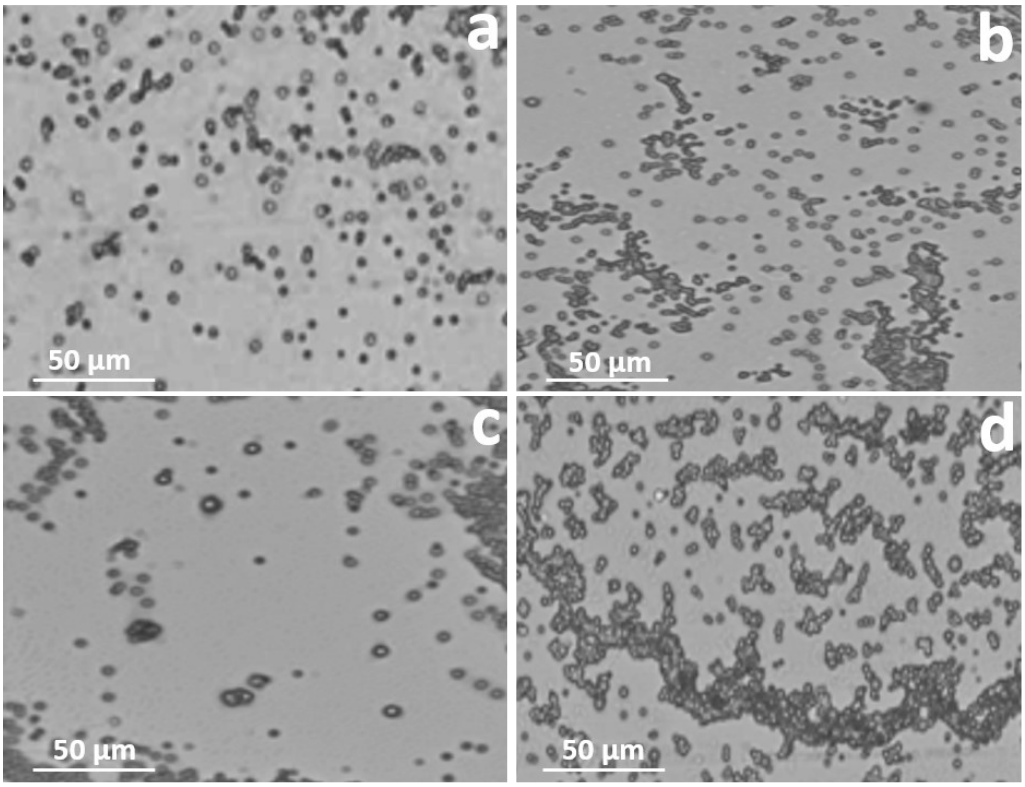

Fig. S24 Optical microscopy images of **Fmoc-Tyr(tBu)-OH** (3 mM) at RT when co-incubated with urea (a) **Fmoc-Tyr(tBu)-OH** under bright field; (b) with urea in 1:1 ratio; (c) with urea in 1:3 ratio; (d) with urea 1:5 ratio.

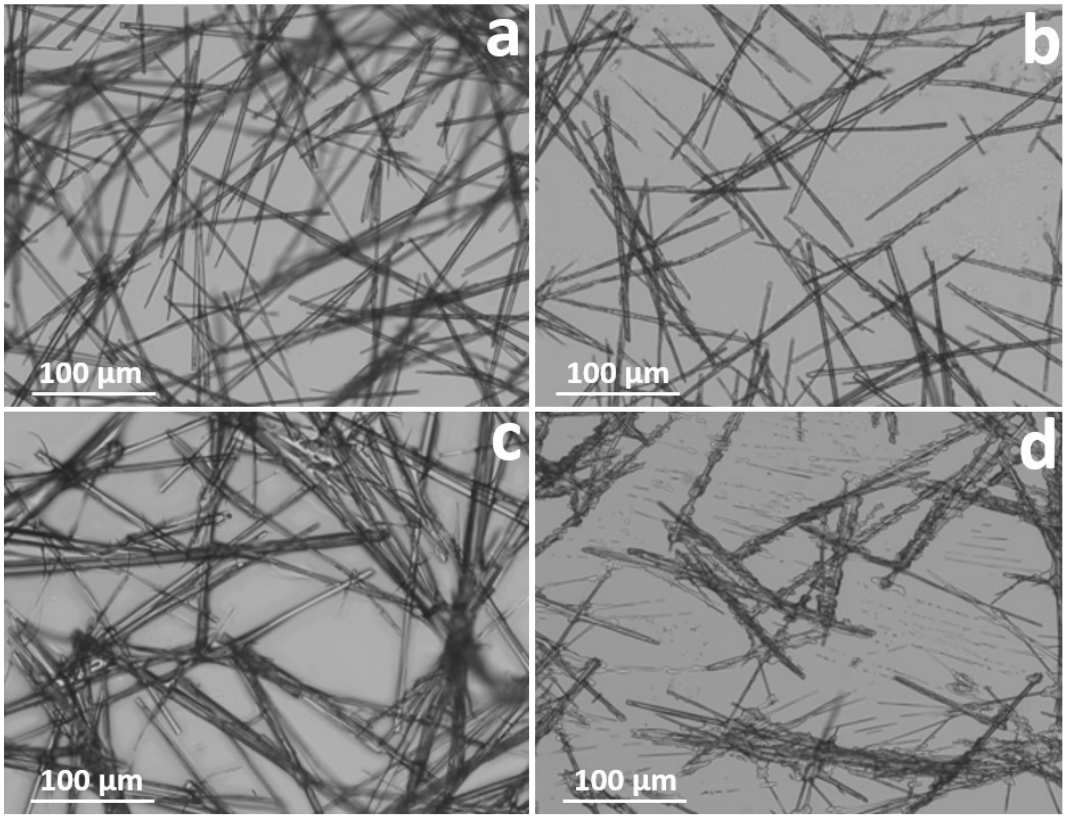

Fig. S25 Optical microscopy images of **Fmoc-Tyr(tBu)-OH** (3 mM) on heating at 70 °C when co-incubated with urea (a) **Fmoc-Tyr(tBu)-OH** under bright field; (b) with urea in 1:1 ratio; (c) with urea in 1:3 ratio; (d) with urea 1:5 ratio.

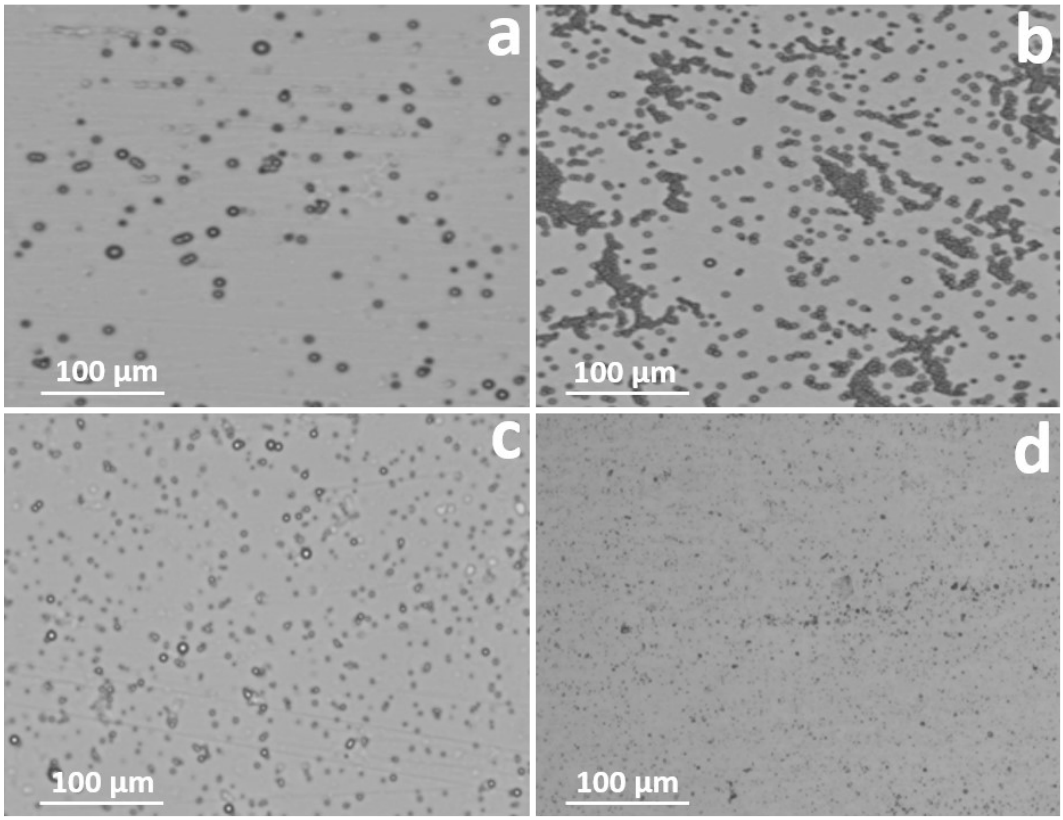

Fig. S26 Optical microscopy images of **Fmoc-Lys(Boc)-OH** (10 mM) on heating at 70 ^{0}C under varying pH (a) at pH 7; (b) at pH 3; (c) at pH 5; (d) at pH 8.

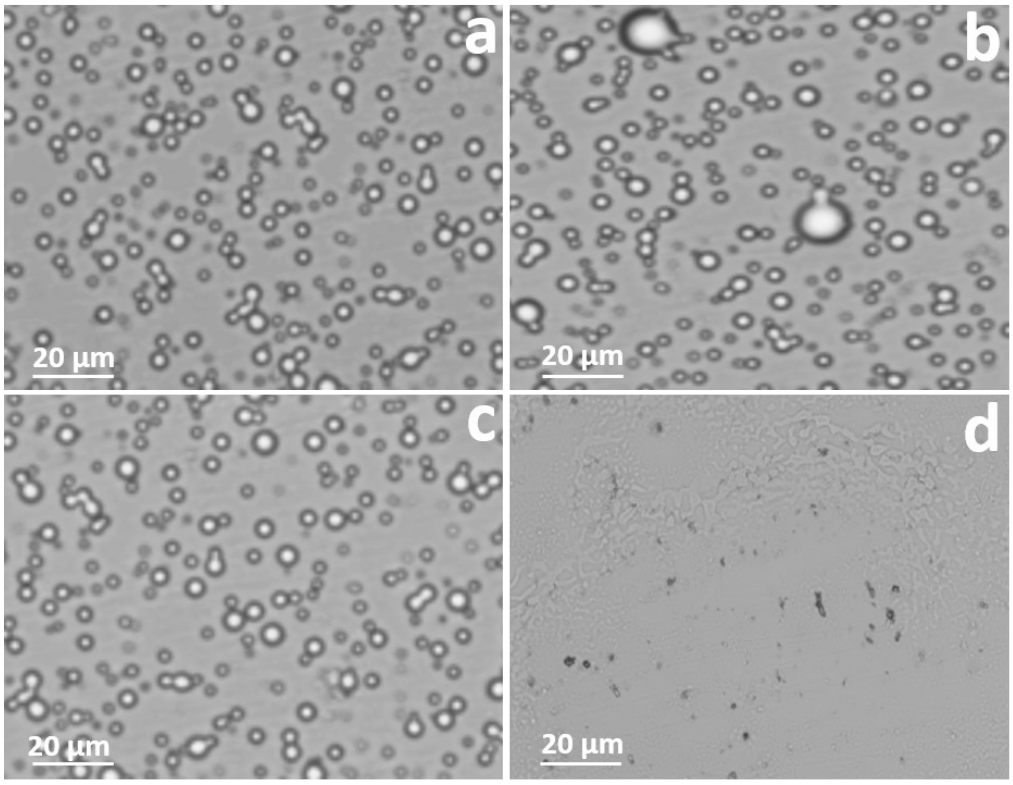

Fig. S27 Optical microscopy images of **Fmoc-Glu(OtBu)-OH** (3 mM) at RT under varying pH (a) at pH 7; (b) at pH 3; (c) at pH 5; (d) at pH 8.

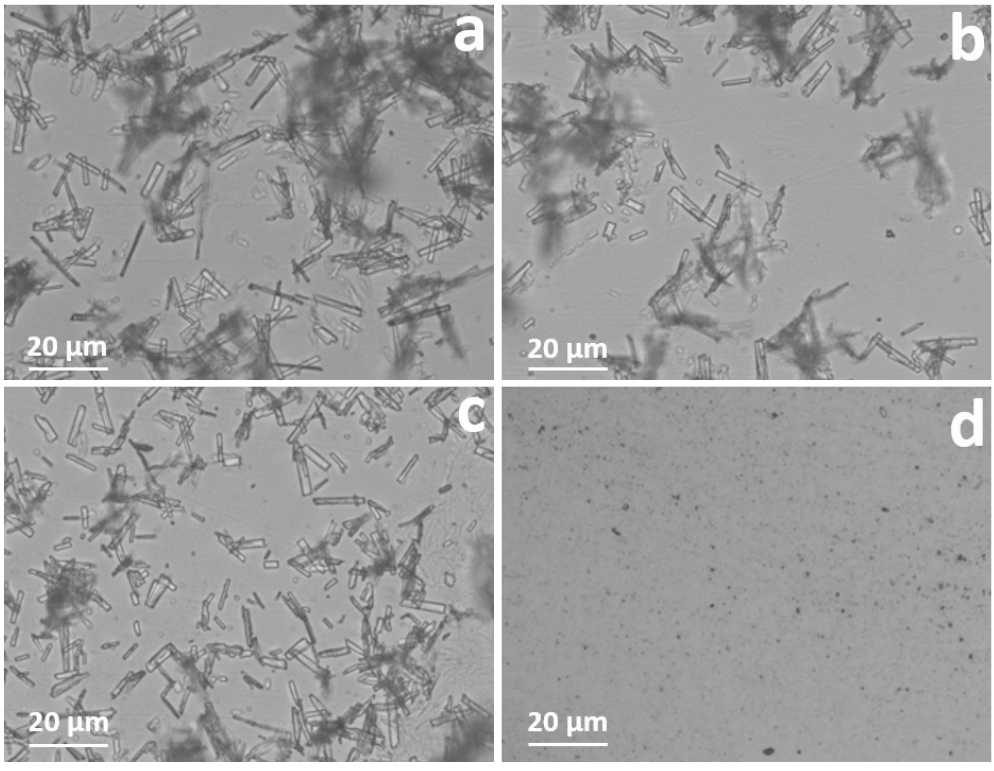

Fig. S28 Optical microscopy images of **Fmoc-Asp(OtBu)-OH** (3 mM) at RT under varying pH (a) at pH 7; (b) at pH 3; (c) at pH 5; (d) at pH 8.

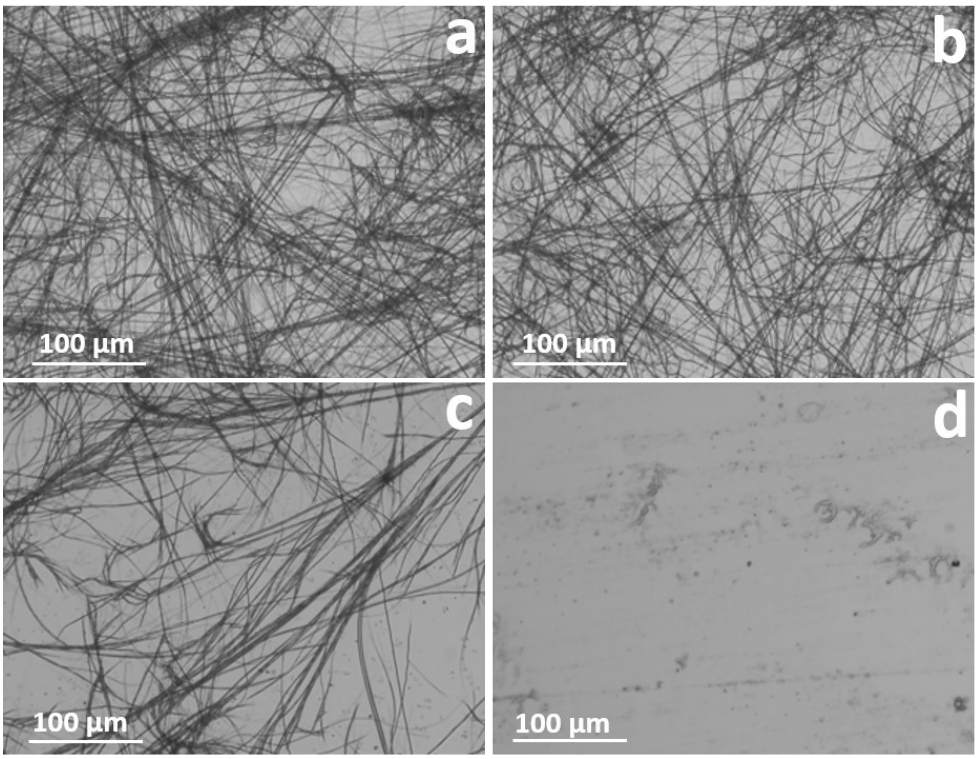

Fig. S29 Optical microscopy images of **Cbz-Phe-OH** (3 mM) at RT under varying pH (a) at pH 7; (b) at pH 3; (c) at pH 5; (d) at pH 8.

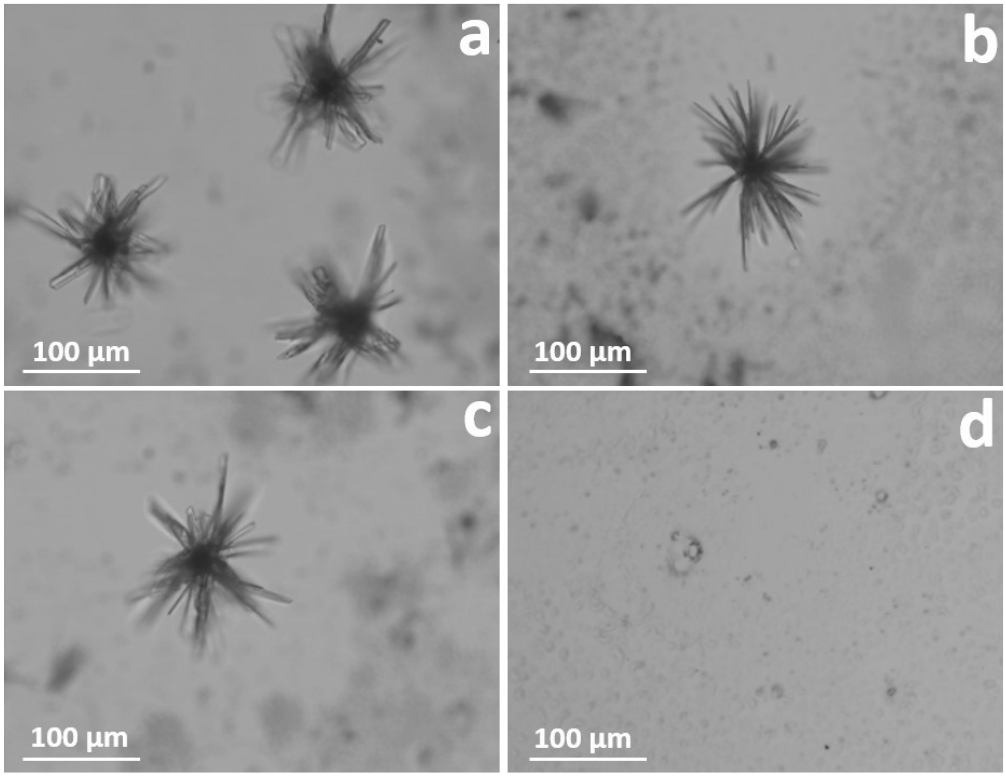

Fig. S30 Optical microscopy images of **Cbz-Trp-OH** (3 mM) at RT under varying pH (a) at pH 7; (b) at pH 3; (c) at pH 5; (d) at pH 8.

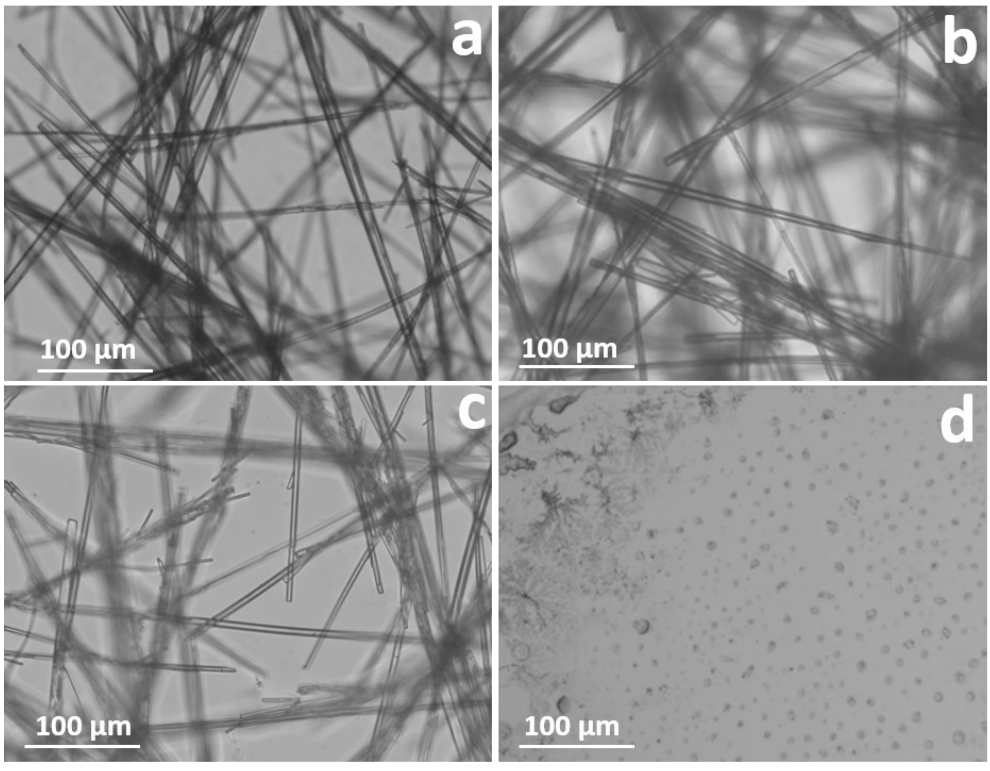

Fig. S31 Optical microscopy images of **Fmoc-Tyr(tBu)-OH** (3 mM) at RT under varying pH (a) at pH 7; (b) at pH 3; (c) at pH 5; (d) at pH 8.

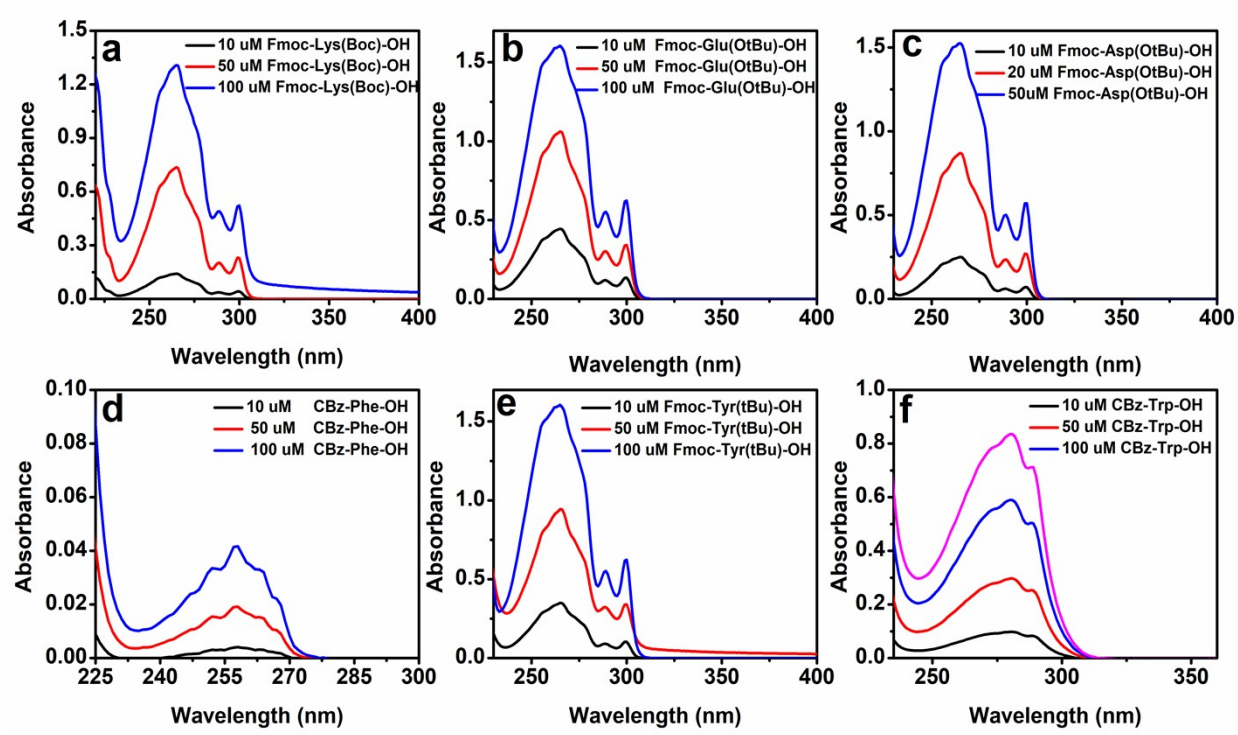

Fig. S32 UV-Visible spectra of modified single amino acids at 10, 50 and 100 µM concentration (a) **Fmoc-Lys(Boc)-OH**; (b) **Fmoc-Glu(OtBu)-OH**; (c) **Fmoc-Asp(OtBu)-OH** ; (d) **Cbz-Phe-OH**; (e) **Fmoc-Tyr(tBu)-OH**; (f) **Cbz-Trp-OH**.

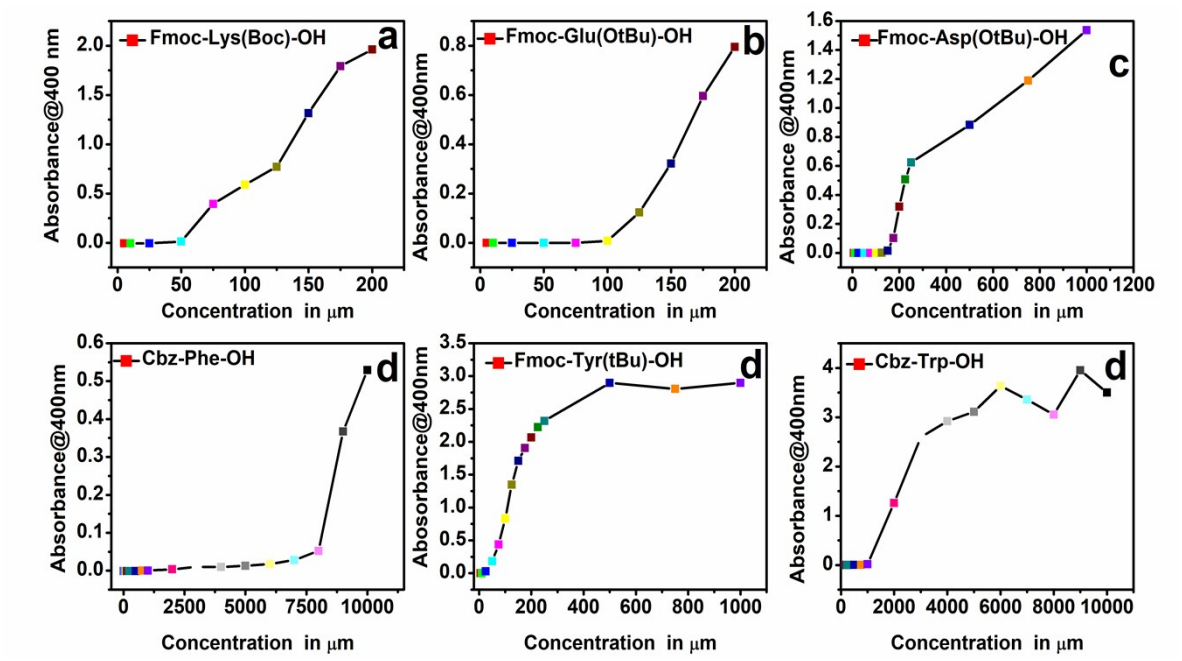

Fig. S33 Turbidity assays of modified single amino acids (a) **Fmoc-Lys(Boc)-OH**; (b) **Fmoc-Glu(OtBu)-OH**; (c) **Fmoc-Asp(OtBu)-OH**; (d) **Cbz-Phe-OH**; (e) **Fmoc-Tyr(tBu)-OH**; (f) **Cbz-Trp-OH**.

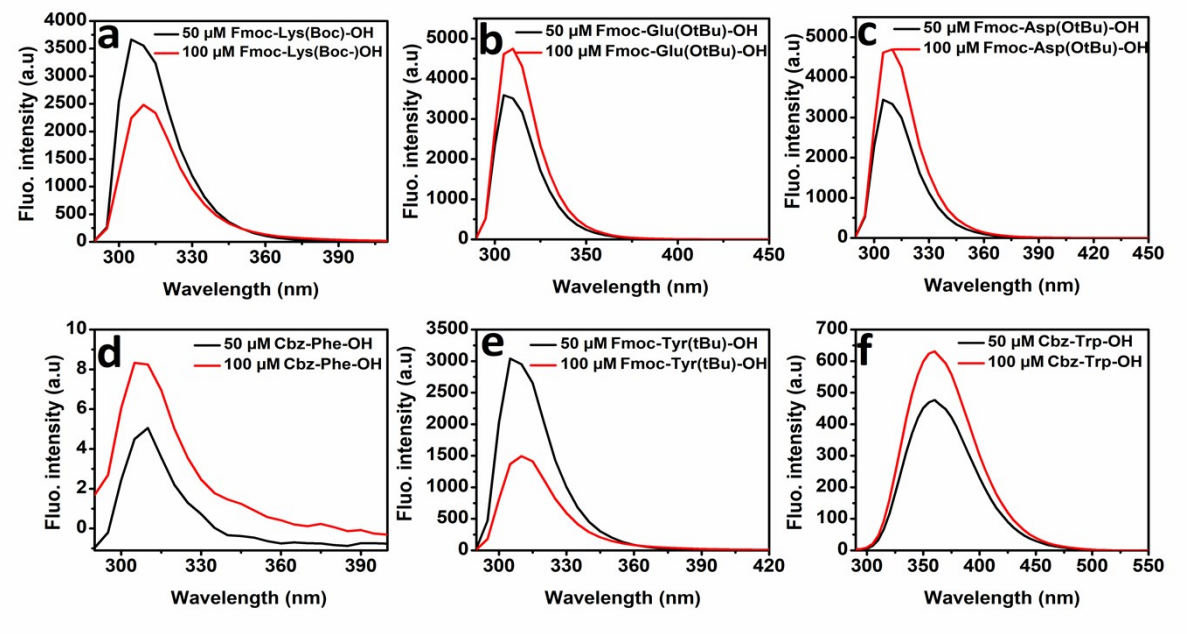

Fig. S34 Fluorescence spectra at 50 and 100 μM concentration excitation@290 (a) **Fmoc-Lys(Boc)-OH**; (b) **Fmoc-Glu(OtBu)-OH**; (c) **Fmoc-Asp(OtBu)-OH**; (d) **Cbz-Phe-OH**; (e) **Fmoc-Tyr(tBu)-OH**; (f) **Cbz-Trp-OH**.

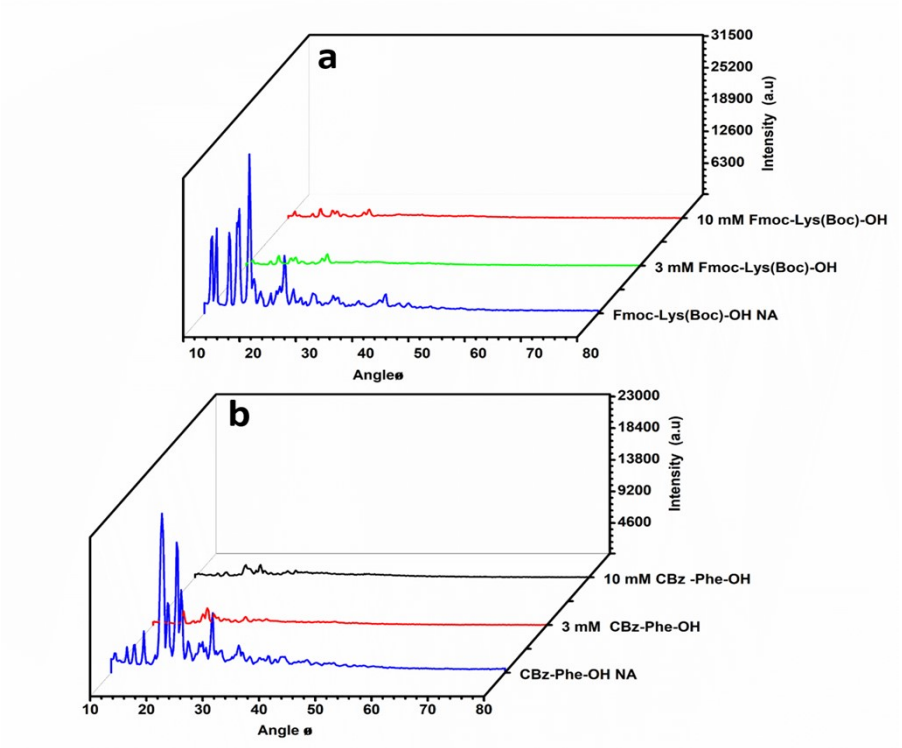

Fig. S35 XRD diffractogram of **Fmoc-Lys(Boc)-OH** and **Cbz-Phe-OH** and 3 and 10 mM demonstrated that broadening and vanishing of the diffraction peak after self-assembly indicating a change in molecular packing and a transition from crystalline to an amorphous state. (a) **Fmoc-Lys(Boc)-OH**; (b) **Cbz-Phe-OH.**

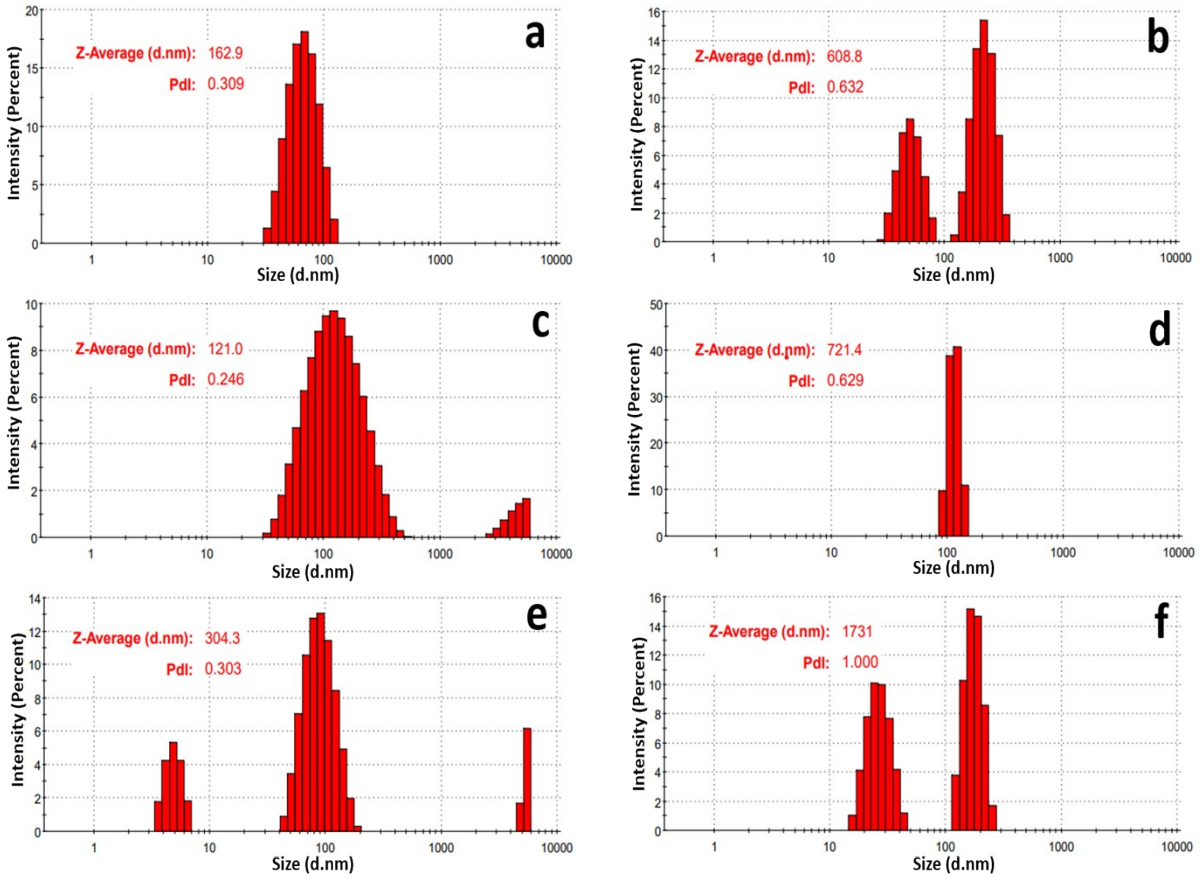

Fig. S36 Dynamic light scattering at 100 µM concentration in water (a) **Fmoc-Lys(Boc)-OH**; (b) **Fmoc-Glu(OtBu)-OH**; (c) **Fmoc-Asp(OtBu)-OH**; (d) **Cbz-Phe-OH**; (e) **Cbz-Trp-OH**; (f) **Fmoc-Tyr(tBu)-OH**.

^{1}H-NMR **studies explanation:** Further, to get insights into the mechanism of self-assembly we also performed concentration-dependent solution state ^{1}H-NMR in DMSO-d6 and subsequently the experiment was done by the addition of drop of D_2O. It was necessary to use DMSO, since the solvent used for self-assembly i.e water and methanol resulted in very turbid solution wherein NMR could not be recorded. Hence, DMSO solvent was used to make conjugates soluble. The concentration-dependent ^{1}H-NMR study of **Cbz-Phe-OH** was performed as representative for all Cbz modified single aromatic amino acids while **Fmoc-Lys(Boc)-OH** was studied as representative for all charged aliphatic single amino acids. The studies were performed at concentrations 1, 3, 5, 7, and 9 mg/mL in DMSO-d6 at ambient temperature. The results reveal that when we increase the concentration the peak broadening

has been observed at 7.19-7.36 ppm in the aromatic region, although no significant shifting was observed. While the -NH proton of carbamate group showed significant deshielding as we increased the concentration of **Cbz-Phe-OH** from 1 to 9 mg/mL in DMSO-d6. The carbamate -NH proton shows a doublet at 7.63 ppm in 1 mg/mL concentration whereas at 9 mg/mL concentration this doublet is shifted to 7.65 ppm which may occur due to the presence of hydrogen bonding.[1, 2]

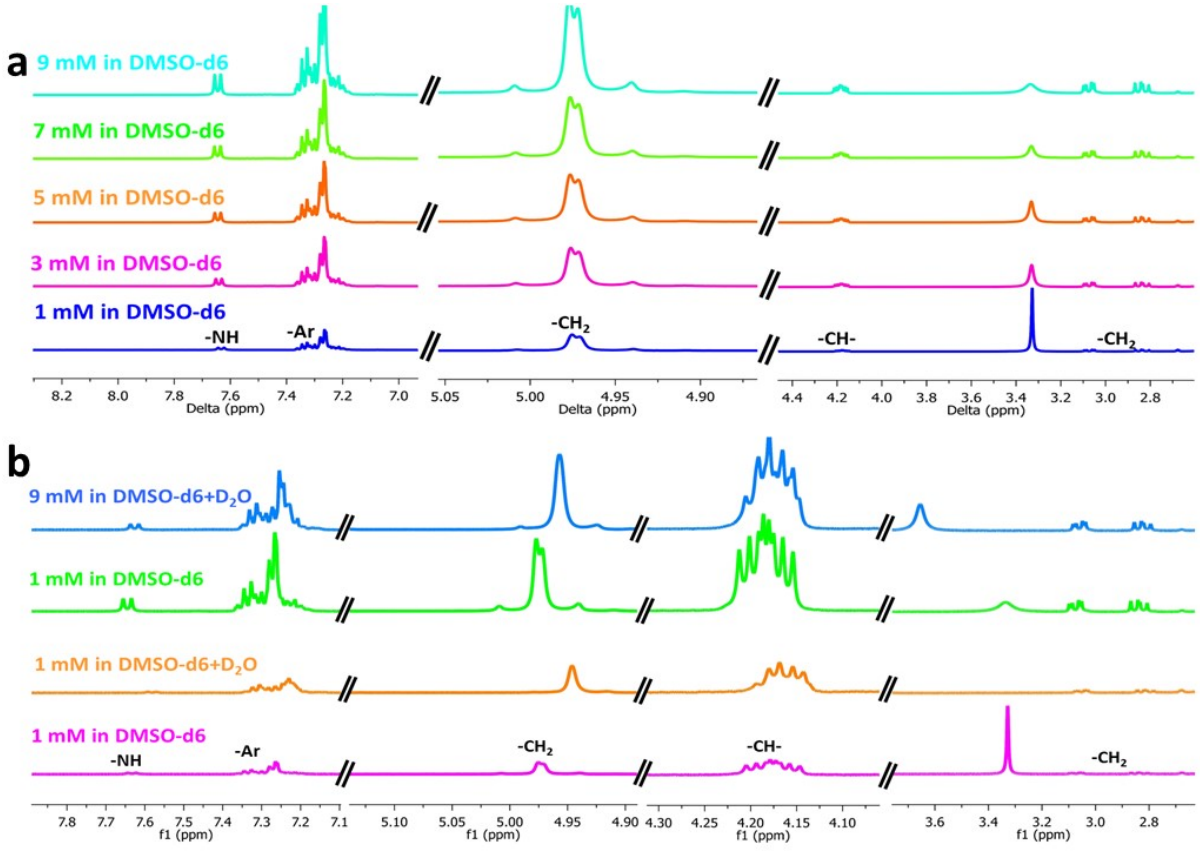

Fig. S37 ^{1}H-NMR spectra of **Cbz-Phe-OH** (a) at concentration 1, 3, 5, 7, and 9 mg/mL in DMSO-d6 (b) ^{1}H-NMR spectra of **Cbz-Phe-OH** at 1 and 9 mg/mL in DMSO-d6 alone and after addition of drop of D_2O respectively

To investigate more about the self-assembled structure formation, we added a drop of D_2O in the DMSO-d6 sample and recorded its ^{1}H-NMR spectra. It was expected that the addition of D_2O will induce more self-assembly. Indeed, after the addition of drop of D_2O the aromatic

peak of **Cbz-Phe-OH** becomes more shielded and revealed upfield shifting which indicated formation of π-π stacking. The aromatic peak in 1 mg/mL **Cbz-Phe-OH** which was observed at 7.17-7.37 ppm was shifted upfield after the addition of D_2O indicating the presence of π-π stacking in the aggregated state due to shielding. Several literature reports implicate the presence of π-π stacking is accompanied by an upfield shifting of the ^1H NMR peaks as more aggregation leads to increased electron density around the nuclei.[3, 4, 5] The comparative analysis of the peak shifting observed with increasing concentration of **Cbz-Phe-OH** in DMSO-d6 and after the addition of a drop of D_2O are presented in table 1.

Table 1: ^1H NMR peak value of **Cbz-Phe-OH** in ppm in DMSO-d6 and after the addition of a drop of D_2O.

Concentration of sample in mg/mL	**Characteristic peak**	**Peak value (ppm) In DSMO-d6**	**Peak value (ppm) after addition of a drop of D_2O in DMSO-d6 sample**
1	Aromatic	7.26 (m)	7.23 (m)
	-NH	7.63 (d)	7.58 (d)
3	Aromatic	7.28 (m)	7.26 (m)
	-NH	7.64 (d)	7.57 (d)
5	Aromatic	7.28 (m)	7.26 (m)
	-NH	7.64 (d)	7.60 (d)
7	Aromatic	7.28 (m)	7.25 (m)
	-NH	7.65 (d)	7.61 (d)
9	Aromatic	7.28 (m)	7.25 (m)
	-NH	7.65 (d)	7.63 (d)

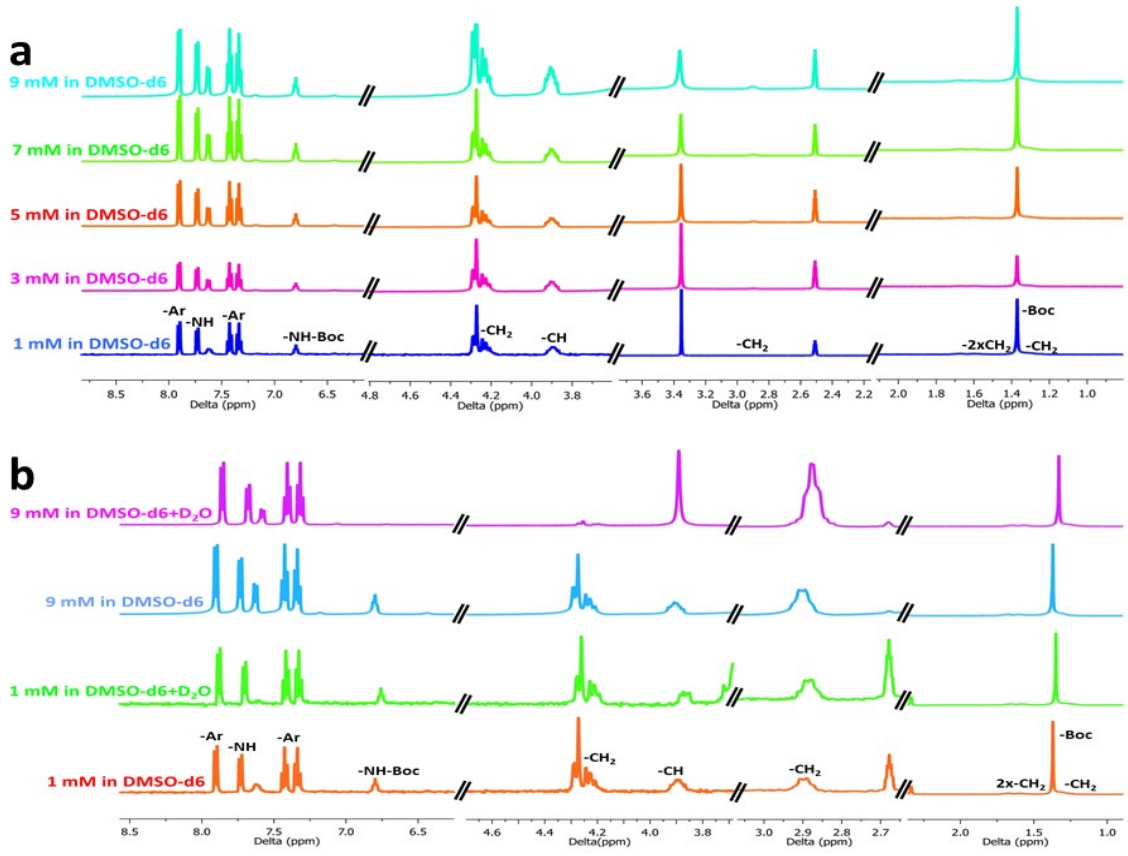

Fig. S38 ^{1}H-NMR spectra of **Fmoc-Lys(Boc)-OH** (a) at concentration 1, 3, 5, 7, and 9 mg/mL in DMSO-d6 (b) ^{1}H-NMR spectra of **Fmoc-Lys(Boc)-OH** at 1 and 9 mg/mL in DMSO-d6 alone and with addition of drop of D_2O.

The concentration dependent ^{1}H-NMR was also performed for **Fmoc-Lys(Boc)-OH** at 1, 3, 5, 7 and 9 mg/mL in DMSO-d6. The study demonstrated that as we increased the concentration from 1 to 9 mg/mL in DMSO-d6, no promising peak shift could be identified (Fig. 7a-7c), instead only some broadening could be observed which indicated that there might be absence of self-assembled structures in DMSO-d6. Hence, a drop of D_2O was added to **Fmoc-Lys(Boc)-OH** sample to induce self-assembly as done in previous study with **Cbz-Phe-OH**. Herein too, we could observe peak shifting after addition of D_2O (Fig. 7d-7f). The aromatic protons of **Fmoc-Lys(Boc)-OH** showed an upfield shift in comparison to **Fmoc-Lys(Boc)-OH** in DMSO-d6 alone, which indicated the self-assembled structures might form due to the presence of π- π stacking which resulted in shielding of nuclei.[6] The aliphatic protons also revealed deshielding effects which may be due to the electrostatic interactions of

Fmoc-Lys(Boc)-OH molecules as we increased the concentration from 1 mg/mL to 9 mg/mL after the addition of drop of D_2O. The details of each peak at 1 mg/mL and 9 mg/mL in DMSO-d6 and DMSO-d6+D_2O have been mentioned in the table 2.

Table 2: ^1H NMR peak values of **Fmoc-Lys(Boc)-OH** in ppm in DMSO-d6 and on the addition of a drop of D_2O.

Types of Protons	**Peak value in ppm 1 mg/mL**	**Peak value in ppm 1 mg/mL+D_2O**	**Peak value in ppm 9 mg/mL**	**Peak value in ppm 9 mg/mL+D_2O**
Acid	12.82	-	12.59	-
Aromatic proton	7.91-7.89, 7.74-7.72, 7.45-7.41, 7.35-7.32,	7.89-7.87, 7.71-7.70, 7.44-7.40, 7.35-7.31,	7.91-7.89, 7.74-7.72, 7.44-7.41, 7.36-7.32,	7.87-7.85, 7.69-7.67, 7.43-7.39, 7.34-7.30,
Carbamate Proton (Boc & and Fmoc)	7.62, 6.81	6.76,	7.64-7.62 6.81-6.78	7.59-7.57
Aliphatic Protons	4.29-4.23, 3.90, 2.89, 2.68-2.67, 2.34-2.33, 1.67-1.64,	4.28-4.21, 3.87, 2.88, 2.68, 2.34-1.70	4.29-4.21, 3.93-3.87, 2.91-2.89,	4.27-4.18, 2.88-2.87, 1.67-1.49
Boc protons	1.43-.1.21	1.56-1.35	1.70-1.31	1.38-1.17

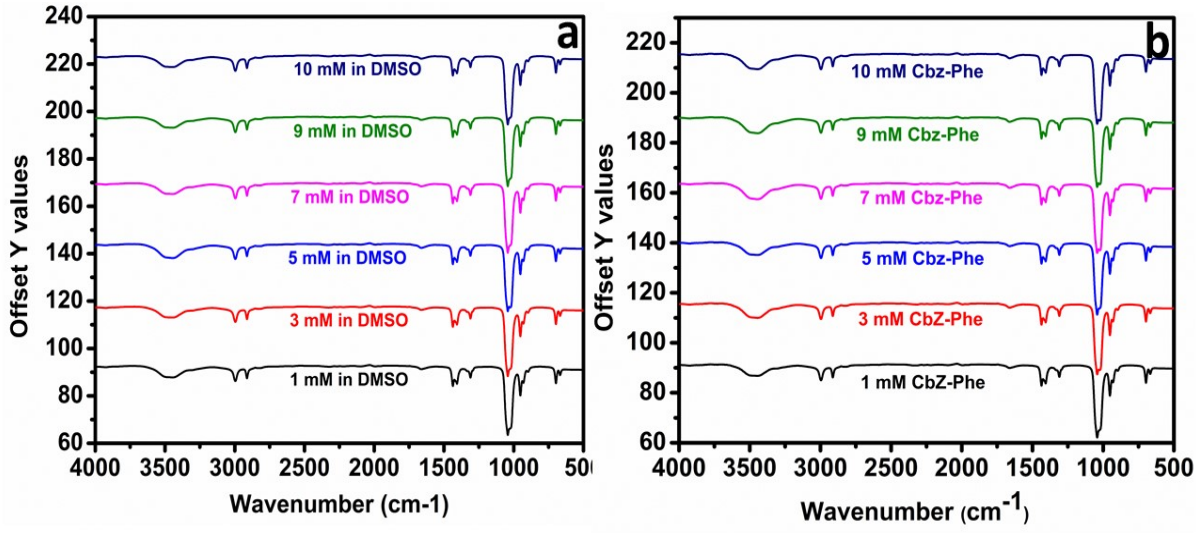

Fig. S39 Full ATR-FTIR spectra modified single amino acids in DMSO (a) **Fmoc-Lys(Boc)-OH**; (b) **Cbz-Phe-OH**.

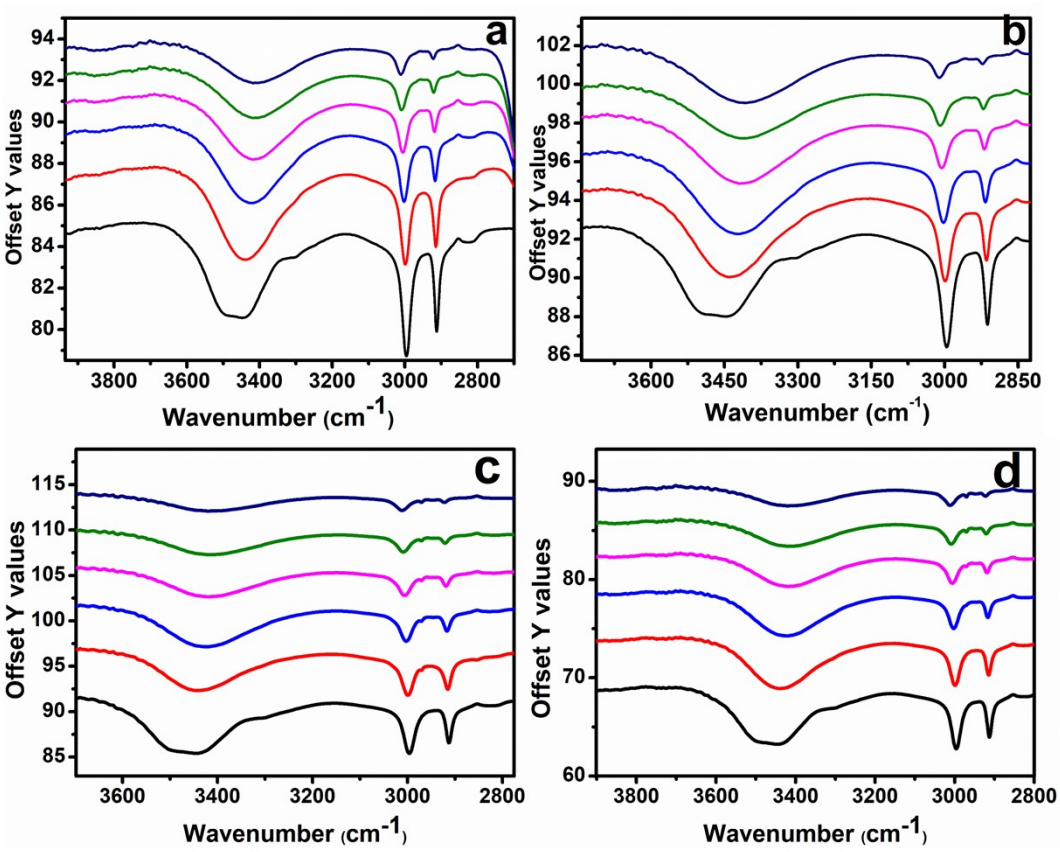

Fig. S40 (a) ATR-FTIR expansion spectra of **Fmoc-Lys(Boc)-OH** at 3 mM concentration in DMSO after addition of 10-50 % D_2O; (b) ATR-FTIR expansion spectra of **Fmoc-Lys(Boc)-OH** at 10 mM concentration in DMSO with addition of 10-50 % D_2O; (c) ATR-FTIR expansion spectra of **Cbz-Phe-OH** at 3mM concentration in DMSO with addition of 10-50 % D_2O; (d) ATR-FTIR expansion spectra of **Cbz-Phe-OH** at 10 mM concentration in DMSO with addition of 10-50 % D_2O.

Reference:

1. A. L. Moraczewski, L. A. Banaszynski, A. M. From, C. E. White and B. D. Smith, *J. Org. Chem.*, 1998, **63**, 7258-7262. DOI: https://doi.org/10.1021/jo980644d
2. A. Syamakumari, A. P. Schenning and E. Meijer, *Chem. Eur. J*, 2002, **8**, 3353-3361. DOI: https://doi.org/10.1002/1521-3765(20020802)8:15<3353::AID-CHEM3353>3.0.CO;2-X
3. V. Kshtriya, B. Koshti, A. Gangrade, A. Haque, R. Singh, K. B. Joshi, D. Bhatia and N. Gour, *New J. Chem*, 2021, **45**, 17211-17221. DOI: https://doi.org/10.1039/D1NJ03269K
4. N. Amdursky and M. M. Stevens, *Chemphyschem*, 2015, **16**, 2768-2774. DOI: https://doi.org/10.1002/cphc.201500260
5. A. C. Boccia, V. Lukeš, A. Eckstein-Andicsová and E. Kozma, *New J. Chem*, 2020, **44**, 892-899. DOI: https://doi.org/10.1039/C9NJ05674B
6. A. Paul, G. Jacoby, D. Laor Bar-Yosef, R. Beck, E. Gazit and D. Segal, *ACS nano*, 2021, **15**, 11854-11868. DOI: https://doi.org/10.1021/acsnano.1c02957